

1 Minimizing the effects of Pb-loss in detrital and igneous U-Pb zircon 2 geochronology by CA-LA-ICP-MS

3
4 Erin E. Donaghy¹, Michael P. Eddy¹, Federico Moreno², Mauricio Ibañez-Mejía²
5 ¹Department of Earth, Atmospheric, and Planetary Sciences, Purdue University, West Lafayette, 47907, United
6 States of America
7 ²Department of Geosciences, University of Arizona, Tucson, 85721, United States of America

8
9 *Correspondence to:* Erin E. Donaghy (edonaghy@purdue.edu)

10 **Abstract.** Detrital zircon geochronology by laser ablation-inductively coupled plasma-mass spectrometry (LA-ICP-
11 MS) is a widely-used tool for determining maximum depositional ages, sediment provenance, and reconstructing
12 sediment routing pathways. Although the accuracy and precision of U-Pb geochronology measurements has improved
13 over the past two decades, Pb-loss continues to impact the ability to resolve zircon age populations by biasing affected
14 zircon toward younger apparent ages. Chemical abrasion (CA) has been shown to reduce or eliminate the effects of
15 Pb-loss in zircon U-Pb geochronology, but has yet to be widely applied to large-n detrital zircon analyses. Here, we
16 assess the efficacy of the chemical abrasion treatment on zircon prior to analysis by LA-ICP-MS and discuss the
17 advantages and limitations of this technique in relation to detrital zircon geochronology. We show that i) CA does not
18 systematically bias LA-ICP-MS U-Pb dates for thirteen reference materials that span a wide variety of crystallization
19 dates and U concentrations; ii) CA-LA-ICP-MS U-Pb zircon geochronology can reduce, or eliminate, Pb-loss in
20 samples that have experienced significant radiation damage; and iii) bulk CA prior to detrital zircon U-Pb
21 geochronology by LA-ICP-MS improves the resolution of age populations defined by ²⁰⁶Pb/²³⁸U dates
22 (Neoproterozoic and younger) and increases the percentage of concordant analyses in age populations defined by
23 ²⁰⁷Pb/²⁰⁶Pb dates (Mesoproterozoic and older). The selective dissolution of zircon that has experienced high degrees
24 of radiation damage suggests that some detrital zircon age populations could be destroyed or have their abundance
25 significantly modified during this process. However, we did not identify this effect in either of the detrital zircon
26 samples that were analyzed as part of this study. We conclude that pre-treatment of detrital zircon by bulk CA may be
27 useful for applications that require increased resolution of detrital zircon populations and increased confidence that
28 ²⁰⁶Pb/²³⁸U dates are unaffected by Pb-loss.
29

30 31 1. Introduction

32 Detrital zircon U-Pb geochronology is a widely-used tool with a broad range of applications across multiple
33 subdisciplines of geology. As the efficiency, accuracy, and precision of U-Pb geochronology measurements continue
34 to improve (e.g., Carrapa, 2010; Gehrels, 2012; Gehrels, 2014; Pullen et al., 2014; Sundell et al., 2021), the production
35 of large detrital zircon datasets by laser ablation-inductively coupled plasma-mass spectrometry (LA-ICP-MS) has
36 become more common. In basin analysis and tectonics, these datasets are often used to determine sediment
37 provenance, characterize source terranes, estimate maximum depositional ages, and reconstruct ancient sediment
38 routing pathways (Fedo et al., 2003; Anderson 2005; Smith et al., 2023). The resulting data is typically interpreted
39 using kernel density estimates (KDEs) or probability density plots (PDPs) and assessed by comparing the means,

Deleted: Increased accuracy and precision in igneous and detrital zircon geochronology using CA-LA-ICPMS

Deleted: p

Deleted: Neoproterozoic to present zircon

Formatted: Superscript

Formatted: Superscript

Deleted: the

Deleted:

Deleted: age populations

Formatted: Superscript

Formatted: Superscript

Deleted: potential

Deleted: , and ongoing research aims to test this method's impact on improving the precision and accuracy of maximum depositional age (MDA) estimations

Deleted: s

Formatted: Superscript

Formatted: Superscript

Deleted: common

Deleted: and widely-used

54 heights, widths, and modes of peaks in detrital zircon age spectra using similarity/dissimilarity metrics. One factor
 55 that may limit the resolution of these peaks is Pb-loss which can smear zircon age populations toward younger apparent
 56 U-Pb dates. This issue may not bias data in which Pb-loss is a recent phenomenon provided that the $^{207}\text{Pb}/^{206}\text{Pb}$ date
 57 is used for zircon crystallization. However, protracted or complicated histories of Pb-loss can make it difficult to
 58 interpret $^{207}\text{Pb}/^{206}\text{Pb}$ dates (Nemchin and Cawood, 2005) and many labs only use this system to constrain a zircon
 59 crystallization date if it is concordant. The precision of the $^{207}\text{Pb}/^{206}\text{Pb}$ chronometer also typically limits its use to
 60 Mesoproterozoic and older zircon. The most precise date for Neoproterozoic or younger zircon is generally obtained
 61 with the $^{206}\text{Pb}/^{238}\text{U}$ chronometer and these dates are more susceptible to open-system behavior. Zircon age populations
 62 that are affected by Pb-loss in this age range can be difficult to identify since Pb-loss trajectories closely follow
 63 Concordia and may result in analyses that are concordant within analytical uncertainty but have spuriously young
 64 $^{206}\text{Pb}/^{238}\text{U}$ dates. This is especially problematic for the estimation of maximum depositional ages (MDAs) in detrital
 65 zircon datasets where age estimations utilize low-n clusters of the youngest zircon ages (Dickinson and Gehrels, 2009;
 66 Herriott et al., 2019; Coutts et al., 2019; Sharman et al., 2020; Vermeesch, 2021). The effect of Pb-loss on detrital
 67 zircon analyses is consequently two-fold. It reduces the number of concordant Mesoproterozoic and older zircons,
 68 making populations in this age range more difficult to identify, and it will cryptically smear Neoproterozoic and
 69 Phanerozoic zircon age populations along concordia toward spuriously young dates, making it difficult to resolve
 70 differences between distinct but similarly aged populations.

71 While high temperature metamorphism may lead to zircon recrystallization and partial, or total, resetting of
 72 the U-Pb system, most Pb-loss in zircon that is hosted in sedimentary strata represents a low temperature process.
 73 Damage to the zircon crystal lattice occurs during each alpha emission along the ^{238}U , ^{235}U , and ^{232}Th decay chains as
 74 the heavy nucleus recoils (Bateman, 1910; Dickin, 2005; Nasdala et al., 2005; Reiners, 2005). At temperatures below
 75 200°C this damage cannot anneal and begins to accumulate (Marsellos and Garver, 2010; Ginster et al., 2019). Areas
 76 where high levels of damage have accumulated are then susceptible to Pb-loss (Chakoumakos et al., 1987; Mattinson
 77 et al., 1994; Garver and Kamp, 2002; Widmann et al., 2019; McKanna et al., 2023). The mechanisms through which
 78 Pb becomes mobile in metamict zircon grains remain understudied, but likely include mobility in low-temperature
 79 aqueous fluids (Goldich and Mudrey, 1972; Black, 1987; Kramers et al., 2009; Keller et al., 2019), which allows water
 80 to penetrate highly radiation damaged zircon and mobilize radiogenic Pb by changing its redox state (Kramers et al.,
 81 2009). Thus, the zircons that are most susceptible to Pb-loss at low temperatures are those that spend long durations
 82 at shallow crustal levels and encounter low-temperature aqueous fluids, both of which are conditions seen by detrital
 83 zircon hosted in sedimentary basins.

84 The chemical abrasion method, in which thermally annealed zircon is partially dissolved in hydrofluoric acid
 85 (HF) prior to analysis has been shown to successfully mitigate low-temperature Pb-loss (e.g., Mundil et al., 2004;
 86 Mattinson, 2005; Widmann et al., 2019; Sharman and Malkowski, 2023) and is widely used in isotope dilution-thermal
 87 ionization-mass spectrometry (ID-TIMS) U-Pb zircon geochronology (see reviews in Schoene, 2014; Schaltegger et
 88 al., 2015). The technique likely benefits analyses in two ways. First, it selectively dissolves zones of the zircon crystal
 89 that have experienced extensive radiation damage and possible Pb-loss (Widmann et al., 2019; McKanna et al., 2023).
 90 Second, the partial dissolution process dissolves inclusions that may harbor non-radiogenic Pb, leading to a higher

Deleted: , but

Deleted: are based off

Deleted: cluster of

Deleted: not

Deleted: (references)

Deleted: (references)

Deleted: s

Deleted: s

Deleted:

Deleted: and incipient weathering

Deleted: , mayb

Deleted: . One model for low temperature Pb-loss centers around the

Deleted: loss of water from microcapillaries in zircon during uplift, and when Pb is exposed to fluids, it becomes mobile and leads to Pb-loss

Deleted: Goldich and Mudrey, 1972;

Deleted: e more(?).

Deleted:

110 proportion of zircon-hosted radiogenic Pb (Pb*) in the measured analysis. Over the last decade, several groups have
111 analyzed chemically abraded zircon by LA-ICP-MS and shown that this approach can successfully mitigate Pb-loss,
112 ~~and results in increased concordance, precision, and, presumably, accuracy of U-Pb dates (Crowley et al., 2014; Von~~
113 ~~Quadt et al., 2014).~~ These results suggest that chemical abrasion prior to large-n detrital zircon analyses may also be
114 useful when the resolution of closely spaced Neoproterozoic and Phanerozoic peak age populations is desired or when
115 high degrees of discordance obscure the interpretation of Mesoproterozoic and older age populations. Here, we assess
116 the benefits and drawbacks of this pre-treatment with a particular focus on whether the resolution of younger zircon
117 age populations is increased, whether it improves concordance for Precambrian detrital zircon populations, and/or
118 whether the selective removal of metamict zircon will bias age populations.

Deleted: resulting

Deleted: the

119 2. U-Pb Zircon Geochronology Approach and Methods

Deleted: ¶

120 We have divided our study into three distinct parts. First, we compare chemically abraded and untreated
121 zircon from 13 zircon reference materials (Table 1) to test whether chemical abrasion systematically biases U-Pb dates
122 analyzed by LA-ICP-MS. Crowley et al. (2014) demonstrated that chemically abraded zircon ablate more slowly and
123 experience greater down-hole fractionation than untreated zircon. These differences are likely related to ~~changes in~~
124 the ability of the laser to couple with zircon that has been etched by the chemical abrasion process. While no negative
125 effects of chemical abrasion were seen in Crowley et al. (2014) or von Quadt et al. (2014), provided that chemically
126 abraded reference materials were used ~~for instrument calibration,~~ we have expanded the age range of reference zircon
127 analyzed to encompass 28.5 – 3467 Ma. This increased age range of the tested reference materials provides a more
128 complete understanding of LA-ICP-MS U-Pb systematics on chemically abraded zircon and whether a single primary
129 ~~reference material~~ can be used ~~to calibrate the instrument~~ for a wide range of zircon dates. Second, we assess the
130 ability of chemical abrasion to mitigate Pb-loss in an igneous sample that has experienced substantial radiation damage
131 by comparing chemically abraded and non-chemically abraded ²⁰⁶Pb/²³⁸U LA-ICP-MS zircon analyses to a newly
132 produced CA-ID-TIMS reference date for ~~a Mesoproterozoic granite~~. Finally, we assess how CA affects detrital zircon
133 (DZ) age spectra by comparing chemically abraded and untreated aliquots of two detrital samples. One sample is
134 Cenozoic in age and contains both Phanerozoic (100-300 Ma) and Precambrian (1000-1200 Ma) zircon age
135 populations, whereas the second sample is Proterozoic and contains zircon age populations between 2000-3500 Ma.
136
137

Deleted: differences

Deleted: in

Deleted: as primary standards

Deleted: standard

Deleted: and U content

Deleted: the same sample

Table 1. Zircon reference materials for U-Pb isotopic analyses

Name	ID-TIMS age (Ma)	2 σ	References	Host lithology	Quantity
Fish Canyon Tuff	28.476	0.029	Schmitz and Bowring (2001) ^{b, c}	Dacite	Unlimited
GHR1	48.106	0.023	Eddy et al. (2019) ^b	Rapakivi Granite	Unlimited
49127	136.6		Gehrels et al. (2008) ^b		Uncertain
Plesovice	337.13	0.37	Slama et al. (2008) ^a	Potassic Granulite	Unlimited
Temora 2	418.37	0.14	Mattinson (2010) ^a	Gabbro	Unlimited
R33	420.53	0.16	Mattinson (2010) ^a	Monzodiorite	Unlimited
SLM	563.5	3.2	Gehrels et al. (2008) ^b	Single Crystal	Limited
SLF	555.86	0.68	Wang et al. (2022) ^b	Single Crystal	Limited
91500	1065.4	0.3	Wiedenbeck et al. (1995) ^b	Single Crystal	Limited
FC1	1098.47	0.16	Mattinson (2010) ^a	Gabbro	Unlimited
Oracle	1434	8	Gehrels et al. (2008) ^b	Granite	Unlimited
QGNG	1851.6	0.6	Black et al. (2004) ^b	Quartz gabbro gneiss	Uncertain
OG1	3467.05	0.63	Stern et al. (2009) ^a	Diorite	Unlimited

^a Chemical abrasion CA-ID-TIMS

^b Traditional ID-TIMS

^cCA-ID-TIMS analyses by Wotzlaw et al. (2013) show significant age dispersion in Fish Canyon Tuff relative to original U-Pb ID-TIMS date of Schmitz and Bowring (2001).

Table 1. Zircon reference materials for U-Pb

Name	ID-TIMS age (Ma)	2 σ
Fish Canyon tuff	28.476	0.0
GHR1	48.106	0.0
49127	136.6	
Plesovice	337.13	0.3
Temora 2	418.37	0.1
R33	420.53	0.1
SLM	563.5	3.
SLF	555.86	0.6
91500	1065.4	0.
FC1	1098.47	0.1
Oracle	1434	8
QGNG	1851.6	0.
OG1	3467.05	0.6

^a Chemical abrasion CA-ID-TIMS

^b Traditional ID-TIMS

Deleted:

Formatted: Line spacing: 1.5 lines

Deleted:

2.1 Methods for Thermal Annealing and Chemical Abrasion

All chemically abraded zircon aliquots were treated at Purdue University following methods modified from Mattinson (2005) and similar to those described in Eddy et al. (2019). Zircon separates were first thermally annealed in quartz crucibles for 60 hours at 900°C in a muffle furnace and then loaded in 3 mL savillex hex beakers with ~1 mL of 28M HF and 0.1 mL of 8M HNO₃ for bulk chemical abrasion. Four hex beakers were then stacked in the PTFE liner for a 125 mL Parr acid dissolution vessel. To ensure vapor exchange during partial dissolution a small hole was drilled through each beaker cap. The fully assembled Parr acid dissolution vessel was then held at 210°C for 12 hours. Once the chemical abrasion process was completed, the leachate was removed from each beaker using a pipette and the zircons were rinsed three times with H₂O. Chemically abraded aliquots were then sent to the University of Arizona LaserChron Center (ALC) for mounting and LA-ICP-MS analyses. Methods for chemical abrasion of zircon prior to the ID-TIMS analyses reported in this paper are similar to those described above, except individual zircon were chemically abraded in 200 μ L Ludwig style microcapsules and repeatedly rinsed in distilled 7M HCl and ultrapure H₂O prior to spiking and complete dissolution.

2.2 LA-ICP-MS Zircon U-Pb Geochronology

Zircon aliquots were mounted in 2.5-cm-diameter epoxy plugs, polished, and imaged by cathodoluminescence using a Hitachi 3400N SEM and a Gatan Chroma CL system prior to analysis by LA-ICP-MS. Chemically abraded zircon were only mounted with chemically abraded zircon reference materials, while untreated zircon aliquots were mounted with untreated reference materials. U-Pb isotopic analyses were obtained via LA-ICP-MS using a Thermo Element2 single-collector ICP-MS coupled with a Teledyne Photon Machines Analyte G2

172 excimer laser at the ALC. The diameter of the laser spot was set to 30 microns. Elemental- and mass-dependent
173 instrumental fractionation were corrected by bracketing unknown analyses with analyses of primary reference material
174 FC1 following the methods described in Pullen et al. (2018). [Please see supplementary Table S23 for tuning](#)
175 [parameters for the laser and mass spectrometer](#). Only chemically abraded primary [reference materials](#) were used for
176 calibration of chemically abraded samples and only untreated primary [reference materials](#) were used for untreated
177 samples following the recommendations of Crowley et al. (2014). Bracketing [of secondary and tertiary reference](#)
178 [materials](#) occurred every 10-11 analyses [with primary reference materials \(FC1, SLF/SLM, R33\)](#) for the round-robin
179 comparison of zircon reference materials, every 2-3 analyses for igneous zircon analyses, and every 5 analyses for
180 detrital zircon samples. Data reduction was completed using an in-house Matlab script, AgeCalcML v.1.42 (Sundell
181 et al., 2021). This program allows the user to filter data by maximum $^{206}\text{Pb}/^{238}\text{U}$ and/or $^{207}\text{Pb}/^{206}\text{Pb}$ uncertainty
182 (typically set to 10%), reverse discordance (typically 5%), and normal discordance (typically 20%). For the purposes
183 of this study, we de-activated all uncertainty and discordance filters in AgeCalcML and all isotopic data measured via
184 LA-ICP-MS that is [clearly](#) from [ablated zircon](#) are reported in Tables S1-S13. However, age interpretations of igneous
185 and detrital zircon data use filtered data (Tables S16-S21).

186 [Uranium concentrations \(ppm\) reported from routine U-Pb LA-ICP-MS zircon analyses at ALC are](#)
187 [semiquantitative and calibrated by bracketing unknowns with analyses of reference materials with a known average](#)
188 [U concentration. However, since chemical abrasion selectively dissolves high-uranium zones, and thus modifies the](#)
189 [average U concentration of reference materials by an unquantified amount, the reported U concentration values for](#)
190 [reference materials analyzed by traditional \(non-CA\) ID-TIMS may no longer be valid. We found that the primary](#)
191 [reference material SLF had homogenous \$^{238}\text{U}\$ cps \(counts per second\) within individual sessions \(Figs. S15-S17\) for](#)
192 [both the CA and non-CA runs. We interpret this to mean that SLF has a homogenous U concentration \(and radiation](#)
193 [damage\) and that any differences in \$^{238}\text{U}\$ cps for SLF between different analytical sessions are related to changes in](#)
194 [the instrument's sensitivity. As such, we normalize the \$^{238}\text{U}\$ cps for all other grains analyzed in each session to the](#)
195 [average \$^{238}\text{U}\$ cps of SLF across all sessions. Given the potential difference between chemically abraded and untreated](#)
196 [SLF U concentrations, we did this correction independently for treated and untreated grains. Since we do not have U](#)
197 [concentration values for treated and untreated SLF, we center our discussions on relative differences in U](#)
198 [concentration as estimated using the intensity \(in cps\) of the \$^{238}\text{U}\$ beam, rather than quantifying U concentrations.](#)

199 [We used Saylor and Sundell \(2016\) DZstats program to complete a quantitative assessment of the similarity](#)
200 [between treated and untreated aliquots. This program implements five tests to compare large-n geochronologic or](#)
201 [thermochronologic datasets. The tests used in this study are similarity, likeness, and cross-correlation. Results from](#)
202 [all five tests are shown in Supplemental Table S22 for both detrital zircon samples. The similarity coefficient measures](#)
203 [if two samples have similar modal sub-intervals as well as similar proportions of components in each one of those](#)
204 [modes. A value for similarity equal to 1 indicates the samples are identical in both peak modes and proportions,](#)
205 [whereas 0 indicates there is no match between modes and proportions \(Saylor and Sundell, 2016\). This test is useful](#)
206 [in assessing the number of peak age populations \(similar mode intervals\) and how peak heights \(proportion of](#)
207 [components in each mode\) change between two samples. The cross-correlation coefficient is also sensitive to the](#)
208 [presence or absence of peak ages, but also changes due to the relative magnitude and shape of peaks. If a sample](#)

Deleted: standards

Deleted: standards

Deleted: clearly

Deleted: collected

Deleted: during

Deleted: usually

Deleted: on the Element2 in this study are

Deleted: analyses

Deleted: canonical

Deleted: discuss

Deleted: using the relative strength of the

Deleted: fully

Deleted: calculated based on simple reference material-sample bracketing relative to the average U concentration for the primary reference material (FC1). However, not all reference materials have homogenous U concentrations across individual grains and are not appropriate for extrapolation to samples in the reference material-sample bracketing method. Instead, we note that primary reference material SLF was found to have homogeneous ^{238}U cps (counts per second) between and within runs of treated and untreated aliquots (Fig S8). Therefore, we base our observations on the ^{238}U cps for each analysis and normalize to SLF ^{238}U cps for all sessions. For most samples in this study (reference material round robins and detrital zircon samples), individual analyses were completed over numerous runs (2-4). To normalize the sample data to SLF, the ^{238}U cps of individual SLF analyses across all runs were averaged for each treated and untreated aliquot. We also calculated an average SLF ^{238}U cps for each treated and untreated aliquot run. The average SLF ^{238}U cps value for each run was then divided by the average for all runs for treated and untreated aliquots, respectively. The resulting fractionation factor was applied to all samples in each run, thus normalizing the ^{238}U cps of samples to the reference material SLF. Because MIGU-02 data was collected in one run, we use the raw ^{238}U cps values for treated and untreated aliquots. By removing minor variations in sensitivity using this simple approach, we focus our discussion on the effects of chemical abrasion as a function of ^{238}U cps rather than U concentrations (ppm). This approach resolves the possible inaccuracies introduced by the effects that chemical abrasion of reference materials can have on U (semiquantitative) concentrations calculated by simple standard-sample bracketing. ¶

Deleted: statistical

Deleted: statistical

Deleted: discussed in detail

Deleted: within this manuscript

Deleted: perfectly matched

259 shared the same peak ages, peak shapes, and magnitude of peaks, it would have a R^2 value of 1. If no peak ages, peak
260 shapes, and magnitude of peaks are shared, the R^2 value would be 0 (Saylor and Sundell, 2016). Likeness is the
261 complement of the area of mismatch between two detrital zircon spectra, or more simply put the degree of “sameness”
262 between detrital zircon age populations (Satoski et al., 2013). Thus, the likeness test compares the degree of overlap
263 between pairs of PDPs and is a measure of resemblance between proportions of two populations with overlapping
264 ages (Gehrels, 2009; Satoski et al., 2013). Values of likeness that approach 1 indicate that two detrital zircon spectra
265 have a high degree of overlap (Satoski et al., 2013; Saylor and Sundell, 2016).

267 **2.3 Zircon Optical Profilometry**

268 To evaluate the effect of CA on laser ablation excavation rates in zircons, we compared the average depth at
269 increasing ablation times on a series of laser pits on treated and untreated reference materials. This was accomplished
270 by generating ten laser ablation pits with excavation times that increased by three seconds (starting at three and
271 increasing to thirty seconds) in single crystals of treated and untreated grains of zircon reference materials FC1, R33,
272 and SL. The resulting pits were imaged using a Veeco Wyko NT9800 Optical Profilometer and depth maps, 3-D
273 images, and crosscut profiles were created using the Vison software produced by Veeco. The images and profiles
274 allowed for the estimation of pit depths and can be used to calculate excavation rates when combined with the known
275 ablation periods (Fig. 2). Laser ablation pits were also imaged and measured on three treated and five untreated
276 unknowns from sample MIGU-02.

278 **2.4 CA-ID-TIMS Zircon U-Pb Geochronology**

279 Sample MIGU-02, a granitoid from the Guyana Shield, was analyzed by CA-ID-TIMS at Purdue University
280 to provide a reference date to compare the chemically abraded and untreated LA-ICP-MS analyses. Following the
281 chemical abrasion methods described above, individual zircons were spiked with the EARTHTIME ^{205}Pb - ^{233}U - ^{235}U
282 isotopic tracer (Condon et al., 2015; McLean et al., 2015) and loaded into a Parr acid digestion vessel with 28M HF.
283 The vessel was then held at 210°C for 60 hours for zircon dissolution. After dissolution, the samples were dried down
284 and converted to chloride form, by adding 75 μl 7M HCl, reassembling the Parr acid digestion vessel, and holding it
285 at 180°C for 12 hours. After conversion to chloride form, the solution was converted to 3M HCl in preparation for
286 anion exchange chromatography. Pb and U were purified from these solutions using AG-1x8 anion exchange resin
287 following procedures modified from Krogh (1973). The resulting aliquots were dried down to a chloride salt before
288 being dissolved in silica gel, dried onto rhenium filaments, and loaded into an IsotopX Phoenix TIMS for analysis. Pb
289 isotopic measurements were made by peak hopping on a Daly detector and corrected for mass dependent isotopic
290 fractionation using an $\alpha = 0.147 \pm 0.028$ (‰amu) and deadtime = 29.9 ns, derived from repeat measurements of the
291 NBS981 Pb reference material. We assume that all ^{204}Pb is from laboratory contamination and correct for it using a
292 laboratory Pb isotopic composition of $^{206}\text{Pb}/^{204}\text{Pb} = 18.82 \pm 0.74$ (2 σ), $^{207}\text{Pb}/^{204}\text{Pb} = 15.52 \pm 0.63$ (2 σ), $^{208}\text{Pb}/^{204}\text{Pb} =$
293 37.93 ± 1.60 (2 σ) derived from repeat total procedural blank measurements run during 2022. Uranium was run as an
294 oxide (UO_2) and isotopic measurements were made statically using Faraday detectors and corrected for fractionation
295 using the known ratio of $^{233}\text{U}/^{235}\text{U}$ in the EARTHTIME ^{205}Pb - ^{233}U - ^{235}U isotopic tracer (Condon et al., 2015; McLean

Deleted: Laser pit depths produced during data acquisition on unknowns from sample MIGU-02 were also studied. Ten laser ablation pits with excavation times increasing by three seconds (starting at three and increasing to thirty seconds) were made in single crystals of treated and untreated reference materials FC1, R33, and SL.

Deleted: . D

Deleted: average laser ablation

Deleted: were used to calculate excavation rates

Deleted: 3

Deleted: then

307 et al., 2015) and assuming a zircon $^{238}\text{U}/^{235}\text{U}$ value of 137.818 ± 0.045 (Hiess et al., 2012). Data reduction was done
308 using the ET_Redux software package (Bowring et al., 2011) and the decay constants of Jaffey et al. (1971). All
309 isotopic data measured via CA-ID-TIMS are presented in [Supplemental Table S17](#).

310

311 3. Results

312 3.1 CA-LA-ICP-MS U-Pb Geochronology of Zircon Reference Materials

313 Treated and untreated aliquots of thirteen different zircon U-Pb reference materials (Table 1) were analyzed
314 in this study to further assess whether chemical abrasion systematically biases U-Pb dates. The reference materials
315 were analyzed during two round-robin runs [using the approach described above](#). The first run targeted 15 zircon grains
316 from treated and untreated aliquot of reference materials. During the second run, 30 zircon grains were targeted.
317 Because FC1 was used as a primary reference material for calibration of the LA-ICP-MS, approximately 30 FC-1
318 zircons were analyzed during run [one](#) and 87 were analyzed during run [two in both](#) treated and untreated aliquots.

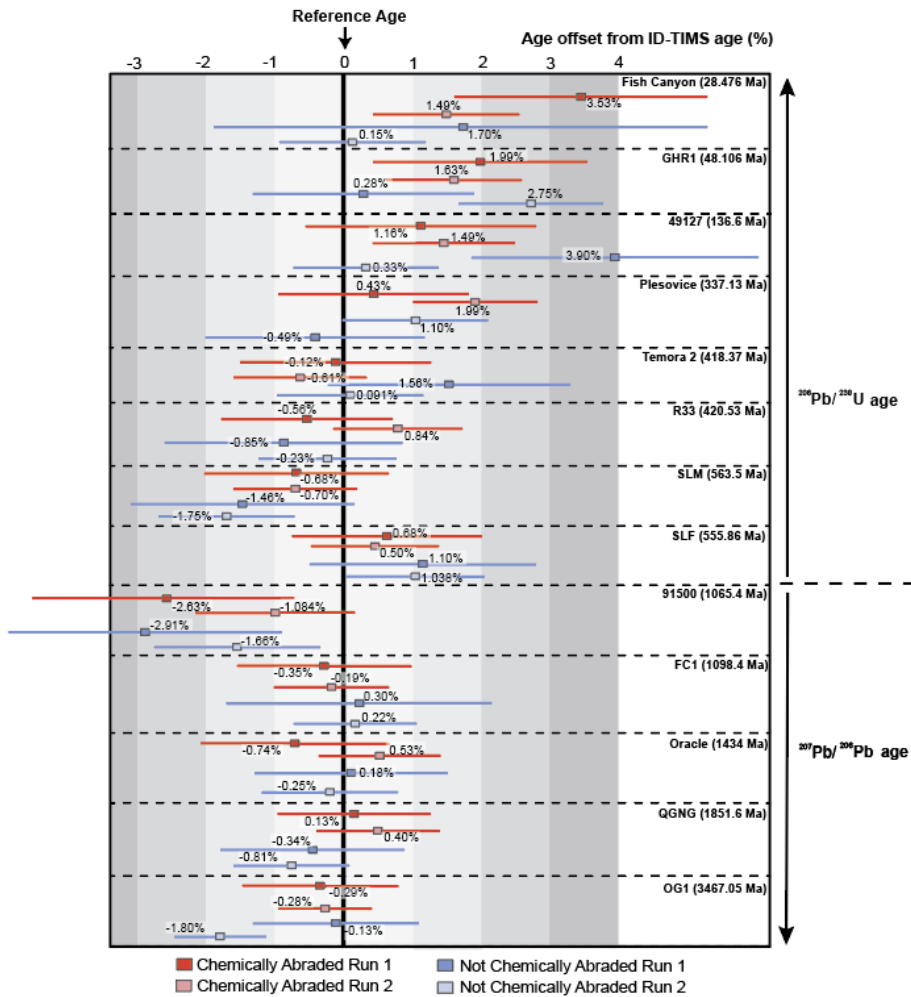
319 [This led to 117 FC1 grains analyzed per treated and untreated aliquots of reference material](#). The total number of
320 zircons analyzed was 653 in each of the chemically abraded and untreated aliquots of reference materials. Of the 653
321 grains in the chemically abraded aliquots, 631 analyses (96.6%) were retained following filtering for discordance,
322 whereas 608 analyses (93.5%) were retained in the untreated aliquot. These results further confirm that CA helps
323 mitigate Pb-loss and improve [the percentage of retained concordant](#) LA-ICP-MS analyses (e.g., Crowley et al., 2014;
324 von Quadt et al., 2014). The most extreme change in concordance and data retention occurred between treated and
325 untreated FC-1 zircon (1098.4 Ma). Of the 117 grains analyzed [in both the](#) treated and untreated aliquots, 99.1% of
326 analyses were retained in the chemically abraded aliquot versus 82.2% in the untreated aliquot. Discordance criteria
327 used for filtering the above data were reverse discordance larger than 5%, $^{206}\text{Pb}/^{238}\text{U}$ errors larger than 10%, [and/or](#)
328 [maximum discordance of over 20%](#). Overall, the discordant FC1 grains in both runs had low U cps and significantly
329 [older \$^{206}\text{Pb}/^{238}\text{U}\$ dates \(>1250 Ma; Fig. S15\)](#).

330 The [weighted mean](#) dates of CA and non-CA reference materials are all within 0.1 – 4% of the reference
331 ages determined by ID-TIMS (Fig. 1). Therefore, [despite an increase in the percent of concordant](#) treated grains
332 relative to untreated grains, weighted means of acceptable analyses are indistinguishable and indicate that it is unlikely
333 that chemical abrasion biases U-Pb dates within LA-ICP-MS instrument uncertainty. [The greatest scatter in calculated](#)
334 [weighted mean ages \(~4 to 0.1% age offset from reference date\) is in both the treated and untreated Mesozoic to](#)
335 [Cenozoic reference materials. Scatter is improved by chemical abrasion in Paleozoic reference materials \(2 to 0.8%](#)
336 [age offset\) and excellent for Proterozoic and Archean aliquots \(0.6 to -0.7%\)](#). Additionally, concordant analyses of
337 [treated](#) aliquots have overall lower ^{238}U cps compared to the untreated aliquots (Fig. S15), [indicating that chemical](#)
338 [abrasion dissolved zones of high U concentrations where Pb-loss is most likely to have occurred \(Widmann et al.,](#)
339 [2019; McKanna et al., 2023\)](#). Since reference materials are selected for their homogeneous isotopic compositions, it
340 is not surprising that [there is similarity in dates between treated and untreated aliquots](#). The reproducibility of U-Pb
341 dates for all of the reference materials is strong evidence that a single primary reference material (FC-1 in this case)
342 can be used to correct for instrumental fractionation across a wide range of zircon ages and trace element compositions
343 for chemically abraded zircon.

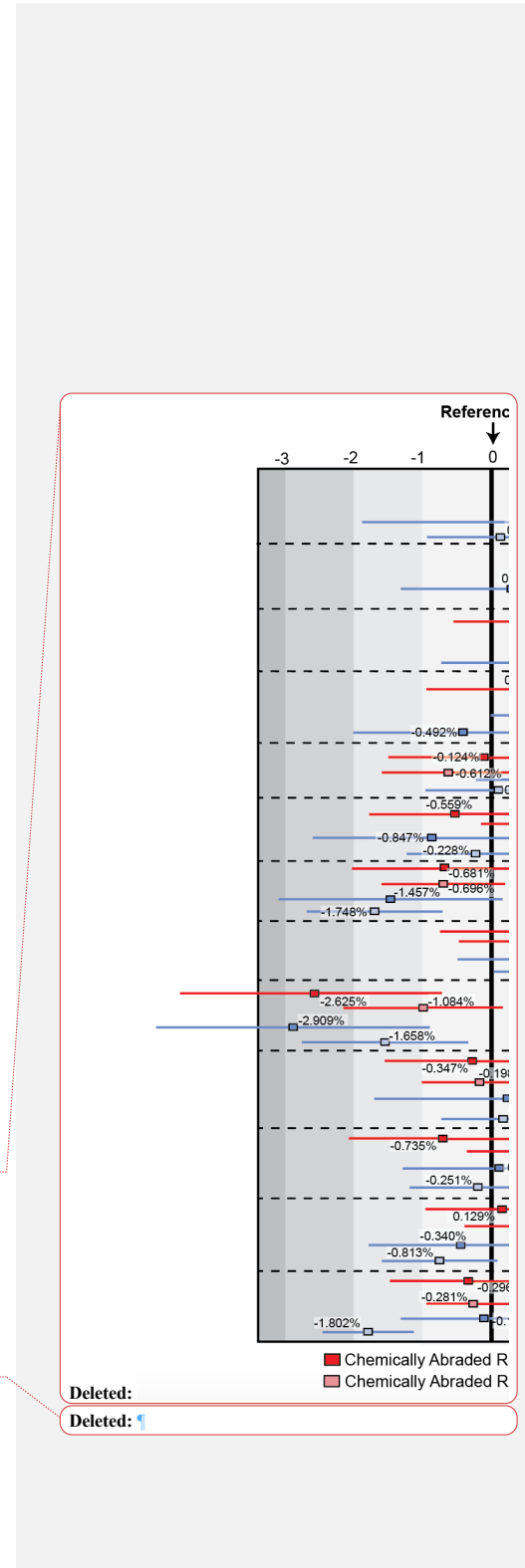
- Deleted: ,
- Deleted: per
- Deleted:
- Deleted: 635
- Deleted: 2
- Deleted: precision in
- Deleted: per
- Deleted: 7.4
- Deleted: 2
- Deleted: 1
- Deleted: and/or
- Deleted: of
- Formatted: Not Highlight
- Deleted:
- Deleted: C
- Deleted: in both treated and un-treated
- Deleted: similar
- Deleted: concentrations
- Deleted: ,
- Deleted: Zones with high U concentrations in zircon are often correlated to zones of radiation damage and Pb-loss (Widmann et al., 2019), and overall lower ^{238}U cps in the treated aliquots suggesting that zones with high U concentrations (Tables S1-S13) were not selectively removed by chemical abrasion (Tables S1-S13; Fig. S15). Although most reference materials have similar scatter in $^{206}\text{Pb}/^{238}\text{U}$ dates, there is despite the correlated reduced scatter in some reference materials (Fish Canyon, GHR1, 49217, Temora 2, R33, SLM, QGNG, and OG1).ion
- Deleted: between high U concentrations, radiation damage, and Pb-loss (e.g., Widmann et al., 2019).
- Deleted: R
- Deleted: However, r
- Deleted: chosen
- Deleted: nature regarding
- Deleted: so
- Deleted: U concentrations are indistinguishable between the two aliquots...
- Deleted: with reduced scatter between individual measurements of the treated aliquot
- Deleted: , U content,

384 Despite the overall similarity in bias between treated and untreated reference materials, the behavior of some
385 reference materials warrants further discussion. The CA-LA-ICP-MS weighted mean $^{206}\text{Pb}/^{238}\text{U}$ dates for two
386 Cenozoic reference materials were older than the CA-ID-TIMS reference date. Chemical abrasion of GHR1 zircon
387 led to an increased proportion of concordant grains, but an older $^{206}\text{Pb}/^{238}\text{U}$ weighted mean date (Fig. S2). We attribute
388 this difference to the presence of slightly older xenocrysts within the sample (e.g., Eddy et al., 2019). We see a similar
389 result for Fish Canyon tuff zircon where the CA aliquot showed increased concordance, but the calculated mean age
390 was offset more from the reference age than the no-CA aliquot (Fig. S1). This sample contains significant antecrysts
391 that might bias its results (e.g., Wotzlaw et al., 2013). Indeed, increased precision and accuracy in analyses of young
392 suites of igneous zircon routinely find overdispersion that can be related to protracted zircon growth or the presence
393 of xenocrysts/antecrysts. Thus, the slight variability in weighted mean dates for GHR1 and Fish Canyon samples in
394 CA-LA-ICP-MS analyses is not entirely unexpected and therefore unlikely to reflect of a systematic bias of the CA-
395 LA-ICP-MS method. Additionally, the 91500 reference material has shown substantial negative age offset in other
396 studies (Gehrels et al., 2008; Schoene et al., 2014), but the origin of these offsets has remained enigmatic, and the
397 offset in this study is not surprising.
398

Deleted: below



400
 401 **Figure 1.** Comparison of $^{206}\text{Pb}/^{238}\text{U}$ and $^{207}\text{Pb}/^{206}\text{Pb}$ (CA)-LA-ICP-MS ages with CA-ID-TIMS ages for thirteen
 402 reference materials that range in age from 28 to 3467 Ma. Each square is the weighted mean of a set of (CA)-LA-ICP-
 403 MS measurements shown as the percent offset from the known reference age (ID-TIMS). The uncertainty is reported
 404 as 2-sigma standard error of the weighted mean. Chemical abrasion of treated aliquots was conducted at Purdue
 405 University and laser ablation analyses were conducted at Arizona LaserChron Center on the Thermo Element2 single-
 406 collector ICP-MS. Methods for LA-ICP-MS at LaserChron using the Element2 are described by Pullen et al. (2018).



409 Variations in laser ablation behavior between primary reference materials used for standardization and
 410 samples is a direct result of differences in zircon matrices and are known as 'matrix effects' (Marillo-Sialer et al.,
 411 2016). Differences in zircon matrices are related to numerous factors (see review in Marillo-Sialer et al., 2016),
 412 including presence/absence of trace elements (Black et al., 2004), the amount of radiation damage (Allen and
 413 Campbell, 2012), and the degree of crystallinity (Steely et al., 2014). These factors all impact the laser's ability to
 414 couple with the surface of the zircon, directly impacting laser ablation rates and the rates of down-hole fractionation.
 415 As a result, matrix-effects can lead to systematic shifts in LA-ICP-MS data and may be a contributor in observed shifts
 416 in treated and untreated aliquots of reference materials in this study (Fig. 1). In order to constrain how CA impacts
 417 laser coupling and ablation rates between treated and untreated reference materials, we ablated 10 spots on a single
 418 treated and untreated zircon crystal of FC1, SL, and R33 (n=60; Table S14). For each individual spot 1-10 on a
 419 reference material, we incrementally raised the ablation duration by 3 seconds (i.e., by 21 individual laser pulses at 7
 420 Hz). This resulted in 10 different spots with ablation durations ranging from 3 to 30 seconds (21 to 210 laser pulses)
 421 and allowed us to calculate laser ablation rates for both treated and untreated zircon. Overall, laser ablation rates varied
 422 linearly with time (0.43 to 0.46 $\mu\text{m}/\text{sec}$) and were similar for treated and untreated aliquots of all primary reference
 423 materials (Fig. 2). Similar ablation rates were observed across all three different treated and untreated aliquots of
 424 primary reference materials. This suggests 1) the primary reference materials have similar zircon matrix densities and
 425 ablate at similar rates (Marillo-Sialer et al., 2014; 2016), and 2) chemical abrasion does not change the zircon matrix
 426 density or alter the zircon surface of primary reference materials in a way that drastically alters laser coupling or
 427 ablation rates.

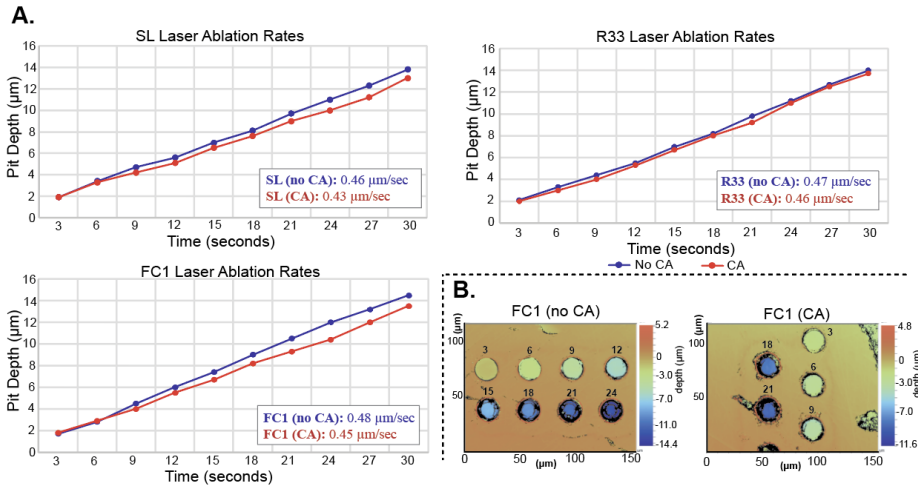
Deleted: can be due to

Deleted: rates

Deleted: 10

Deleted: for each treated and untreated aliquot of FC1, SL, and R33, ...

Deleted: between not only treated and untreated aliquots of the same primary reference materials, but also



428 **Figure 2.** A. Line graphs showing pit depths (μm) versus time (seconds) for unabraded and abraded aliquots of primary
 429 reference materials. Each data point represents an individual pit. Untreated reference materials have slightly deeper
 430 pit depths and ablate at marginally faster rates, but overall, rates of ablation for treated and untreated reference
 431 materials are similar. B. An example of one of the VEECO surface data maps showing pit depths on treated and

Formatted: Font: Bold

Formatted: Font: Bold

Formatted: Indent: First line: 0"

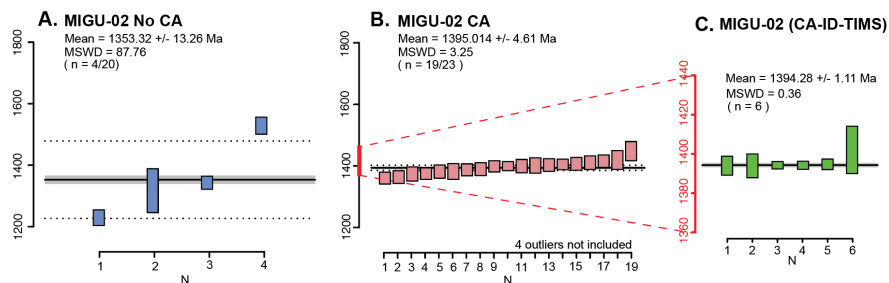
Deleted: are

untreated zircon of FC1. Pits are labeled with the duration in seconds of ablation. See Supplemental Table S14 for all pit depth data from abraded and unabraded reference materials.

3.2 Untreated and CA- U-Pb Zircon LA-ICP-MS Analyses of Metamict Zircon

A Precambrian granite sample from the Parguaza Complex in the North Guyana Shield (MIGU-02; N 5° 21' 3.70"; W 67° 41' 33.41") that has experienced substantial radiation damage was analyzed to assess the effects of chemical abrasion on grains with significant Pb-loss. Untreated (n = 35) and treated aliquots (n = 23) of MIGU-02 were analyzed at the ALC and compared to a reference age determined by CA-ID-TIMS (n=6) at Purdue University (Fig. 3; Tables S14 and S15). During the bulk chemical abrasion process, 80-85% of MIGU-02 grains fully dissolved, leaving only a small fraction of the original aliquot to be used for analyses.

²⁰⁷Pb/²⁰⁶Pb Rank Order Plots



²⁰⁶Pb/²³⁸U Rank Order Plots

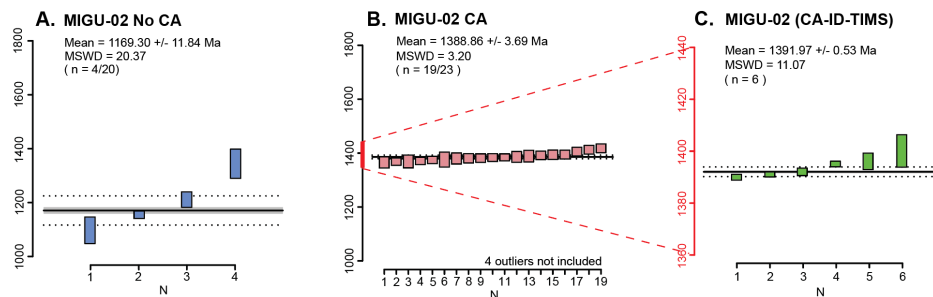


Figure 3. Rank order plots of calculated ²⁰⁷Pb/²⁰⁶Pb and ²⁰⁶Pb/²³⁸U ages for treated and untreated MIGU-02 aliquots and of the reference age for MIGU-02 obtained using CA-ID-TIMS. **A.** Untreated samples of MIGU-02 show large degree of scatter in dates and substantial deviation from the reference age. **B.** Treated zircons show a significant increase in precision and accuracy of ages relative to the reference age. **C.** Reference age for MIGU-02 determined using the weighted mean of six grains. See text for discordance criteria.

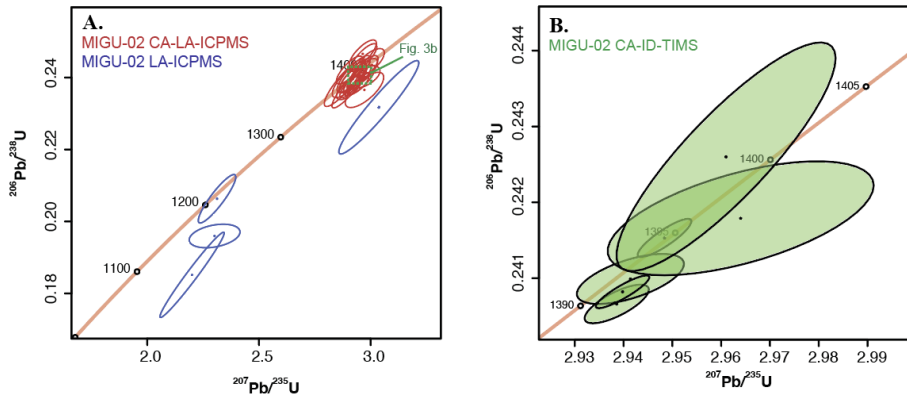
Deleted:
Deleted: 2
Deleted: 1
Deleted: 1
<object>

Deleted: 2

Deleted: 1

464 The $^{207}\text{Pb}/^{206}\text{Pb}$ CA-ID-TIMS reference age for MIGU-02 is 1394.28 ± 1.11 Ma (n=6, MSWD = 0.36),
 465 while the $^{206}\text{Pb}/^{238}\text{U}$ dates are more scattered (Fig. 3). The scatter indicates that U/Pb elemental fractionation occurred
 466 during chemical abrasion in one analysis (slight reverse discordance) and residual Pb-loss remained in others (normal
 467 discordance)(Fig. 4). Nevertheless, a weighted mean date of the $^{206}\text{Pb}/^{238}\text{U}$ CA-ID-TIMS dates is 1391.97 ± 0.53 Ma
 468 (n = 6, MSWD = 11.06) and indicates that residual Pb-loss only affects the dates at the <0.5% level. Untreated LA-
 469 ICP-MS analyses of MIGU-02 show significant discordance (Fig. 4) and only 4 analyses (n=4/20; 80% discordant)
 470 were retained after filtering by AgeCalcML v.1.42. Chemical abrasion substantially increased the number of
 471 concordant analyses (n = 23/23). Fifteen analyses were removed from the untreated aliquot dataset and seven analyses
 472 were removed from the treated aliquot dataset because they hit epoxy and are not included in the totals. Although all
 473 grains were concordant in the treated aliquot, four grains were not included in the weighted mean because they had a
 474 significantly older $^{207}\text{Pb}/^{206}\text{Pb}$ dates (1571-1900 Ma) than the CA-ID-TIMS reference date (Table S14) and are likely
 475 xenocrystic. The weighted mean $^{207}\text{Pb}/^{206}\text{Pb}$ date from the untreated MIGU-02 aliquot is 1353.32 ± 13.26 Ma (n =
 476 4/20; MSWD = 87.76) and the treated aliquot is 1395.014 ± 4.61 Ma (n = 19/23; MSWD = 3.25). The mean $^{206}\text{Pb}/^{238}\text{U}$
 477 date of the untreated aliquot is 1169.30 ± 11.84 Ma (MSWD = 20.37) and the mean $^{206}\text{Pb}/^{238}\text{U}$ date of the treated
 478 aliquot is 1388.86 ± 3.69 Ma (MSWD = 3.20). Thus, the dates from treated zircon show a significant increase in
 479 concordance, precision, and accuracy relative to the reference date as determined by CA-ID-TIMS (Fig. 3).

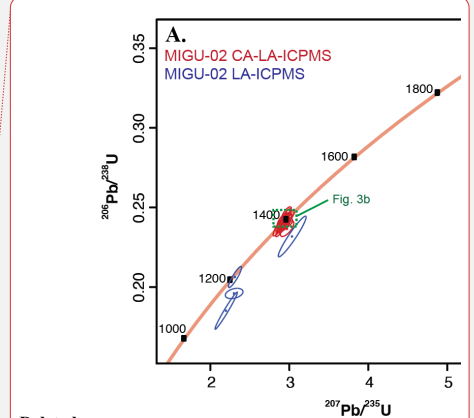
480



481 **Figure 4.** A. Untreated and treated aliquots of MIGU-02 shown on a concordia plot. Non-CA MIGU-02 dates are
 482 discordant whereas CA dates fall on concordia and overlap the reference age. B. All CA-ID-TIMS analyses of MIGU-
 483 02 shown on a concordia plot. One date shows slight reverse discordance whereas all other dates fall on concordia or
 484 have slight normal discordance.

485
 486
 487 All the CA-treated analyses have lower ^{238}U beam intensity than the untreated grains suggesting that CA
 488 selectively removed zones of higher U concentration (Fig. 5). Furthermore, the untreated zircon with the highest ^{238}U
 489 beam intensity are associated with U-Pb dates that are $>\pm 20\%$ discordant (Table S16). Since uranium concentration

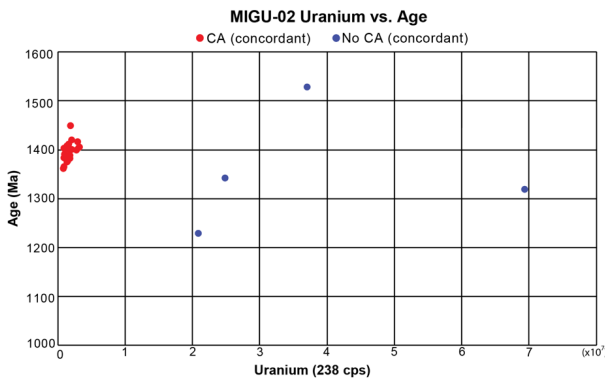
Deleted: 4...2828... +/- 1.111.11...Ma (n=6, MSWD = 0.36), while the $^{206}\text{Pb}/^{238}\text{U}$ dates are more scattered (Fig. 2...). The scatter indicates that U/Pb elemental fractionation occurred during chemical abrasion in one analysis (slight reverse discordance) and residual Pb-loss remained in others (normal discordance)(Fig. 43.... Nevertheless, a weighted mean date of the $^{206}\text{Pb}/^{238}\text{U}$ CA-ID-TIMS dates is $1391.971.97 \dots /- 0.5355 \dots$ Ma (n = 6, MSWD = 11.060.98... and indicates that residual Pb-loss only affects the dates at the <0.5% level. Untreated LA-ICP-MS analyses of MIGU-02 show significant discordance (Fig. 43... and only 4 analyses (n=4/20; 80% discordant) were retained after filtering by AgeCalcML v.1.42. Chemical abrasion substantially increased the number of concordant analyses (n = 23/23). Fifteen analyses were removed from the untreated aliquot dataset and seven analyses were removed from (... [1]



Deleted: 3... A. Untreated and treated aliquots of MIGU-02 shown on a concordia plot. Non-CA MIGU-02 dates are reversely ... (... [2]
 Deleted: When both untreated and treated MIGU-02 dates are plotted against uranium concentration ^{238}U cps, a
 Deleted: uranium concentrations
 Deleted: cps
 Deleted: (<500 ppm)
 Formatted: Superscript
 Deleted: , while untreated grains show significant variation and overall higher ^{238}U cps... in uranium concentration (... [3]
 Deleted: 4
 Deleted: Most ...urthermore, the untreated zircon with the highest of the high (... [4]
 Deleted: uranium concentration
 Deleted: cps... eam intensity analyses come from untreated zircon that ...re associated with U-Pb dates that are $>\pm 20\%$ reversely ...iscordant (Table S16), but these are not shown on Figure 5 due to plot scaling (... [5]

633 is correlated to radiation damage in old zircon, this result reinforces the observation that CA is an effective tool for
 634 removing damaged zones of the zircon (Nasdala et al., 2005; Widmann et al., 2019). Pit depths were measured on five
 635 untreated and three treated zircons from MIGU-02 (Table S15). The average pit depth for untreated grains of MIGU-
 636 02 is ~10.34 μm, whereas it is ~8.1 μm for the treated aliquot. This indicates that the pit depths of the untreated aliquot
 637 of MIGU-02 are ~25% deeper than the treated aliquot and that CA does has an impact on the laser ablation rate in
 638 highly metamict samples.

639 We acknowledge that for samples with significant radiation damage, there is always the possibility that the
 640 entire sample will dissolve during chemical abrasion, and it is up to the researcher to determine if this technique is
 641 appropriate for their objectives. Running a high-n data acquisition on highly damaged zircon might ultimately yield
 642 enough concordant analyses to make a confident age determination, but analyses of MIGU-02 that passed typical
 643 discordance filters were inaccurate by up to -11% for the ²⁰⁷Pb/²⁰⁶Pb dates and -21% for the ²⁰⁶Pb/²³⁸U dates (Fig. 3),
 644 suggesting that even filtered data may be inaccurate for metamict zircon. In contrast, the chemically abraded aliquot
 645 did not have these issues, despite the significant loss of zircon grains during the HF chemical attack.



646 **Figure 5.** Uranium (²³⁸cps) plotted against ²⁰⁷Pb/²⁰⁶Pb age (Ma) for both treated and untreated aliquots of MIGU-02. Only concordant analyses are shown because discordant analyses for MIGU-02 have extremely low ²³⁸U cps. Uranium concentration is directly proportional with radiation damage in zircon with the same low-temperature

659 cooling history. The restricted range of low ²³⁸U cps in the CA-treated grains suggests that CA was effective at
 660 dissolving high U zircon that was more likely to have Pb-loss.

661 **3.3 Untreated and CA- U-Pb Zircon LA-ICP-MS Analyses of Detrital Zircon**

662 One Phanerozoic (NM8A) and one Precambrian sample (Rora Med) were analyzed to determine how detrital
 663 zircon age distributions compare between chemically abraded and untreated aliquots. We followed the ‘Large-n’
 664 approach of Pullen et al. (2014) for both treated and untreated aliquots to obtain a more robust distribution of ages,
 665 their modes, peak widths, and abundances. For NM8A, we analyzed 512 individual zircons in the treated aliquot and
 666 896 zircons in the untreated aliquot. In Rora Med, we analyzed 1035 zircons in the treated aliquot and 920 zircons in
 667 the untreated aliquot. We used Saylor and Sundell (2016) DZstats program to complete a quantitative assessment of
 668 the similarity between treated and untreated aliquots (See definitions described above; Table S22). Additionally, we
 669 calculated the fraction of grains that defined distinct peak age populations in each aliquot to assess how the proportion
 670 of each population changed after chemical abrasion. Our results show that chemical abrasion (CA) changed the number
 671 of each population.

Deleted: ¶

Deleted: concordant

Deleted: for metamict igneous sample MIGU-02

Formatted: Superscript

Formatted: Superscript

Formatted: Superscript

Formatted: Superscript

Deleted: s.

Deleted: ¶

Formatted: Indent: First line: 0"

Deleted: <object>

Deleted: 4

Deleted: concentrations

Deleted: (ppm

Deleted: Both

Deleted: and discordant

Deleted: concentrations

Deleted: in this study

Deleted: in samples with a wide range of age populations

Deleted: for this study

Deleted: ,

Deleted: of all analyzed samples – treated and untreated

Deleted: statistical

Deleted: in Methods

Deleted: also

Deleted: percentage

Deleted: represent out of the total grains

Deleted: the

Deleted: age populations changes

696 and distribution of apparent peak age populations in both DZ samples compared to the non-CA age spectra (Figs. 6
 697 and 7). Most notably, the Phanerozoic age peaks in sample NM8A narrowed, became more defined, and, in some
 698 cases, shifted to slightly older dates.
 699

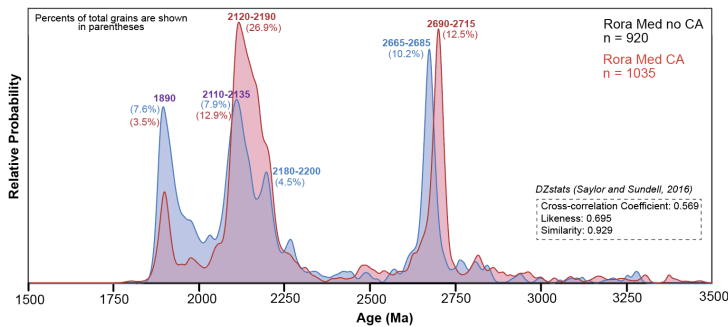


Figure 6. Comparison of U-Pb detrital zircon age spectra of non-chemically abraded (blue) and chemically abraded (red) aliquots of Rora Med. Areas where age spectra overlap are shaded in purple. Quantitative

710 comparisons of treated and untreated aliquots were completed using Saylor and Sundell (2016) DZstats to calculate
 711 cross-correlation, likeness, and similarity values. All quantitative comparison analytics are reported in Table S20. The
 712 percentages above the peaks represent the percentage the peak age population represents out of the total grains. We
 713 aimed for n=1000 for each aliquot because Pullen et al (2014) shows the distribution of analyzed zircon ages is thought
 714 to approach the 'true' age distribution of the sample.
 715
 716

717 In the Precambrian sample (Rora Med), there are subtle changes in the DZ age spectra between the treated
 718 and untreated aliquots. Overall, the CA treated aliquot shows a higher percentage of concordant grains (Fig. 6)
 719 narrower, better defined, peak age populations, changes in the number of peaks present, and a slight but noticeable
 720 shift in peak age populations to older ages (Fig. 6). Of note, the 1890 Ma peak narrows in the treated aliquot compared
 721 to the broad peak that covers a range of ages between 1890 and 2000 Ma in the untreated aliquot. However, the fraction
 722 of grains within this population decreased from 7.6% to 3.5% between the untreated and treated fractions, respectively.
 723 There is also a change in the shape and number of peaks between the two fractions between 2100 and 2300 Ma. In the
 724 untreated aliquot, there are three distinct peak age populations (~2120 (~7.9%), 2190 (~4.5%), & 2260 Ma (<2%)),
 725 whereas in the treated aliquot, there is only one broad peak age population that spans between ~2120-2190 Ma (~30%).
 726 There is also a distinct shift in the untreated aliquot 2675 Ma peak age population to fifteen million years older in the
 727 treated aliquot (Fig. 6). Quantitative comparisons support these observations. A likeness coefficient of 0.695 and
 728 cross-correlation coefficient of 0.569 support there are significant differences in the number, shape, and magnitude of
 729 certain peak age populations. However, a similarity value of 0.929 indicates that even with these changes for specific
 730 age populations, there is an overall high degree of overlap in the number and proportion of modes in the detrital zircon
 731 spectra between treated and untreated aliquots.
 732

Deleted: 5

Deleted: 6

Deleted: 5

Deleted: was

Deleted: improved

Deleted: ce

Deleted: 7

Deleted: and age spectra show narrowing of

Deleted: 5

Deleted: The change in the peak height of the 1890 Ma peak age corresponds to a decrease in the proportion of grains representing that age population between treated and untreated aliquots. The 1890 Ma age population decreases from 7.6% of the total grains in the untreated aliquot to 3.5% in the treated aliquot.

Deleted: treated and untreated aliquots for

Deleted: the

Deleted: -

Deleted: range

Deleted: 15

Deleted: 5

Deleted: Statistical

Deleted: q

756

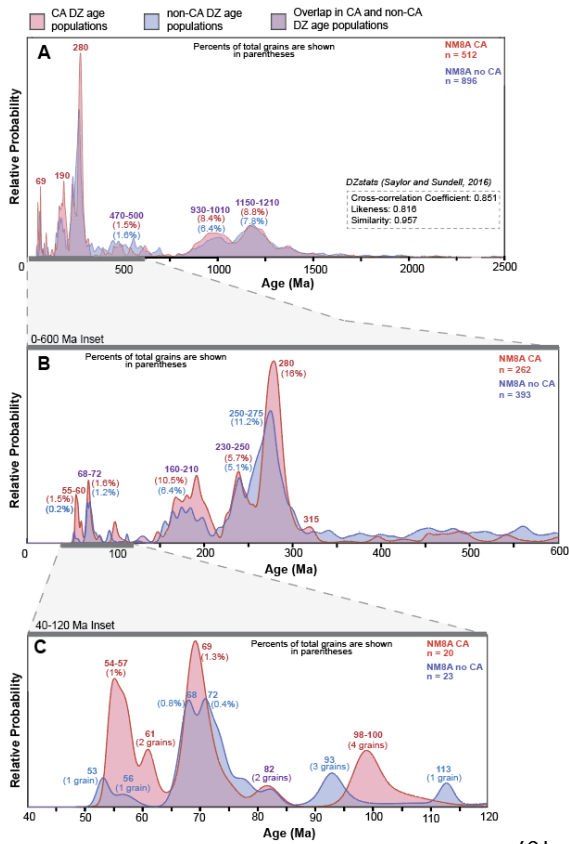


Figure 7. Comparison of U-Pb detrital age spectra of not chemically abraded (blue) and chemically abraded (red) aliquots of NM8A. Areas where age spectra overlap are shaded in purple. Quantitative comparisons of treated and untreated aliquots were completed using Saylor and Sundell (2016) DZstats to calculate cross-correlation, likeness, and similarity values. All quantitative comparison analytics are reported in Table S20. The percentages above the peaks represent the percentage the peak age population represents out of the total grains. We aimed for n=1000 for each aliquot as the distribution of analyzed zircons ages is thought to approach the ‘true’ age distribution of the sample (Pullen et al., 2014). Insets A-C show variations of the scale on the x-axis.

Deleted: <object>
Deleted: 6

Deleted: 2015

782

783

784

785

786

787

788

789

790

791

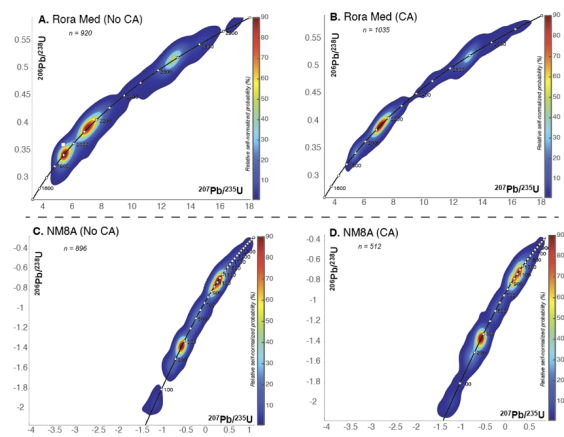
792

There are also subtle changes in the number of peaks and peak shapes between the treated and untreated aliquots of NM8A. The most significant changes observed are increased resolution and definition of Phanerozoic peak age populations in the treated aliquot (Fig. 7). For example, between 200-300 Ma, two broad peaks in the untreated aliquot sharpen and narrow to two well-defined peak age populations in the treated aliquot (Fig. 7b). Additionally, a distinct 190 Ma peak is present in the treated aliquot compared to a broad range of populations between 160 and 210 Ma in the untreated aliquot. We also see a zone of two broadly defined peaks at 68 and 72 Ma in the untreated aliquot sharpen to a singular peak at 69 Ma in the treated aliquot. In the untreated aliquot, the 68-72 Ma age populations make up ~1.2% of the total grains in the untreated aliquot, whereas in the treated aliquot the 69 Ma peak age population represents ~1.3% of total grains. There is also an older shift from the 93 Ma peak in the untreated aliquot to ~98 Ma in the treated aliquot. However, due to the low number of grains within these peak age populations, it is possible these

Deleted: between 0 and 300 Ma for
Deleted: 6
Deleted: (230-250 and 250-275 Ma)
Deleted: 6
Deleted: 50
Deleted: 00
Deleted: sharpens to a more distinct peak at 190 Ma, with two subordinate peaks between 150 and 175 Ma in the treated aliquot.
Deleted: that represent

806 [shifts are related to subtle differences between the two fractions and not a consequence of the chemical abrasion](#)
 807 [process. For example, the peak height change in the 93 Ma population \(3 grains; untreated aliquot\) to the 98-100 Ma](#)
 808 [\(4 grains; treated aliquot\) represents the addition of a single grain \(Fig. 7c\).](#) Other shifts and changes in peak age
 809 populations that are <120 Ma (Fig. 7c) cannot be confidently constrained due to the low number of analyses that define
 810 those populations (1-2 grains). [The fraction of concordant grains is indistinguishable between treated and untreated](#)
 811 [aliquots of NM8A \(Fig. 8\).](#) [Quantitative comparisons of treated and untreated aliquots further support these results](#)
 812 [and similarity, cross-correlation, and likeness values are all >0.8 \(Fig. 6\).](#) The Similarity value of 0.957 indicates a
 813 [strong overlap in the number and proportion of detrital zircon peak age populations overall. Slightly lower, but still](#)
 814 [high, cross-correlation \(0.851\) and likeness \(0.816\) coefficients support minor shifts in the number of peak age](#)
 815 [populations \(modes\) and changes in peak heights \(magnitude\).](#)

- Deleted: just artifacts of peak shapes due to low-n
- Deleted: Most certainly
- Deleted: from
- Deleted: 6
- Deleted: percent
- Deleted: Concordance
- Deleted: 7
- Deleted: The statistical quantification tests for comparison
- Deleted: s



816 **Figure 8.** Density contour concordia diagrams for not chemically abraded and chemically abraded aliquots of detrital zircon samples NM8A and Rora Med (A-D). There is substantial improvement in [the scatter of concordant analyses in the chemically abraded aliquot](#) of the Proterozoic Rora Med sample [compared to the untreated aliquot \(A-B\)](#). However, both aliquots of the Phanerozoic NM8A sample are indistinguishable (C-D). Please note that the concordia diagrams for NM8A (C-D) are plotted on a logarithmic scale [to best display](#)

- Deleted: 7
- Deleted: ce
- Deleted: from the not chemically abraded to the chemically abraded aliquot

831 [the large range Phanerozoic to Precambrian ages.](#)

832 4. Discussion

833 Our study shows that chemical abrasion prior to LA-ICP-MS analysis does not negatively affect resulting U-
 834 Pb dates provided chemically abraded reference materials are used as the primary [reference material for calibration](#),
 835 (e.g., Crowley et al., 2014; von Quadt et al., 2014). We also show that chemical abrasion is extremely effective in
 836 mitigating the effects of Pb-loss in LA-ICP-MS U-Pb dating of zircon that has experienced substantial radiation
 837 damage. Significant improvement was observed in both $^{206}\text{Pb}/^{238}\text{U}$ and $^{207}\text{Pb}/^{206}\text{Pb}$ dates of MIGU-02 zircon relative
 838 to ID-TIMS results, and also the efficiency of the analyses was dramatically improved by focusing LA-ICP-MS
 839 analyses on only those grains/fragments that survived the chemical abrasion process and had not sustained significant
 840 radiation damage. These results reinforce the observations of previous studies that used this approach (Crowley et al.,
 841 2014; von Quadt et al., 2014) and suggested that the CA-LA-ICP-MS method can be valuable for studies that need

- Deleted: standard
- Deleted: ³⁸
- Deleted: U

860 increased precision and accuracy in LA-ICP-MS U-Pb zircon analyses. Although, care must be taken to ensure data
861 is not biased when this pre-treatment is applied.

862 One important consideration is whether chemical abrasion negatively affects the laser ablation process.
863 Variations in laser ablation pit depths have been directly correlated to the density of the zircon matrix (Marillo-Sialer
864 et al., 2014; 2016) and changes in ablation rate change down-hole fractionation. Previous research has indicated that
865 annealing leads to lower ablation rates compared to unannealed zircon and more homogenous rates across annealed
866 zircon with variable initial degrees of radiation damage (Marillo-Sialer et al., 2016). These observations support results
867 from Campbell and Allen (2012) that thermal annealing zircon samples prior to LA-ICP-MS will reduce matrix-related
868 bias and improve accuracy and precision. However, the impact of CA on laser coupling and ablation rates is not as
869 well characterized. Crowley et al. (2014) found that treated zircons had pit depths that were 25% shallower than
870 untreated aliquots of zircons that experienced extensive Pb-loss. This is identical to the results for the metamict MIGU-
871 02 sample in this study in which chemically abraded zircon also had ~25% shallower ablation pits than untreated
872 zircon (Table S15). The shallower pit depths could be driven by less effective laser coupling in treated aliquots due to
873 small-scale etching and creation of a 3-D porous texture by partial dissolution (Crowley et al., 2014). In comparison,
874 laser ablation rates and pit depths in treated and untreated aliquots of primary reference materials were nearly identical
875 (Fig. 2). This supports conclusions drawn by Crowley et al. (2014) that the extent to which zircon is impacted by CA
876 is dependent on U concentration and the presence of physical defects and highlights the importance of incorporating
877 a wide range chemically abraded reference materials in each analytical session.

878 Our data, and the data of Crowley et al. (2014) and von Quadt et al. (2014), indicate that provided care is
879 taken to use chemically abraded reference materials, the pre-treatment will mitigate Pb-loss and lead to increased
880 accuracy in LA-ICP-MS U-Pb zircon analyses. Given this apparent benefit, it is natural to extend the technique to
881 detrital zircon and test the advantages and disadvantages afforded by this method. Crowley et al. (2014) first used this
882 approach on an Archean graywacke and showed that it did not significantly bias their results. However, this technique
883 has not been widely used over the last decade. We report similar results to previous studies in that chemical abrasion
884 does not significantly bias results or negatively affect LA-ICP-MS dates. This is supported by quantitative comparison
885 tests of the treated and untreated aliquots of both detrital zircon samples that show high degrees of similarity between
886 aliquots. Minor changes in cross-correlation and likeness values are a result of minor changes in the number of and
887 magnitude of specific peak age populations between treated and untreated aliquots (Fig. 6 and 7). Our results indicate
888 that a chemical abrasion pre-treatment may help resolve finer scale features in detrital zircon spectra from the Cenozoic
889 to the Archean. We attribute this increased resolution mainly to the mitigation of Pb-loss leading to increased accuracy
890 of the resulting LA-ICP-MS U-Pb dates.

891 The mitigation of Pb-loss is most clearly observed in the sharpening of Neoproterozoic through Cenozoic
892 age populations because $^{206}\text{Pb}/^{238}\text{U}$ dates provide the most precise estimate for zircon crystallization in this age range.
893 Pb-loss can significantly affect the accuracy of dates in this age range since Pb-loss trajectories closely follow
894 concordia and can result in dates that have apparent concordance despite being inaccurate. These effects can be seen
895 most clearly in sample NM8A where age peaks narrowed and became more defined (e.g., 250-300 Ma peak age
896 populations) following chemical abrasion and some peak age populations shifted to slightly older dates (Fig. 7).

Deleted: .

Deleted: .

Deleted: . Lower laser ablation rates in annealed zircons have been observed compared to unannealed zircons due to the increase in density of the crystal structure during the thermal annealing process (850° C for 48 h; Marillo-Sialer et al., 2014). This difference in laser ablation rates impacts the down-hole fractionation rate, making it imperative to compare annealed samples to reference materials treated the same way. Additional research shows that annealing samples at temperatures over 950° C for 36 hrs results in equivalent ablation rates between different zircon matrices, regardless of their initial crystal structure (crystalline to metamict; Marillo-Sialer et al., 2016).

Deleted: is

Deleted: s

Deleted: can

Deleted: laser

Deleted: lesser

Deleted: studied

Deleted: more

Deleted: high alpha-dose zircon

Deleted: our study

Deleted: which

Deleted: the

Deleted: aliquot

Deleted: more

Deleted: .

Deleted: the

Deleted: s of chemical abrasion to LA-ICP-MS analyses

Deleted: statistical

Deleted: We posit that mitigation of Pb-loss is behind the observed s

Deleted: in our samples

Deleted: zircon dates in this age range are best determined using $^{206}\text{Pb}/^{238}\text{U}$

Formatted: Superscript

Formatted: Superscript

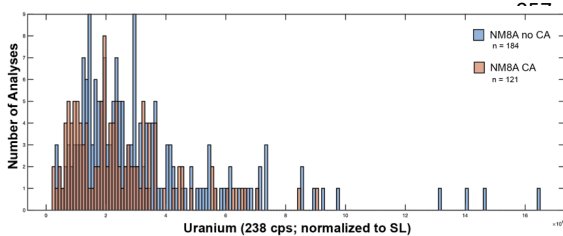
Deleted: U,

Deleted: and the accuracy of this date can be compromised by Pb-loss that is difficult to identify since Pb-loss trajectories for zircon of this age range will closely follow concordia. ...

Deleted: 6

939 Assuming that the zircons that form these populations cooled below the temperature at which radiation damage is
 940 effectively annealed at a similar time, then U content can be used as a proxy for radiation damage (Nasdala et al.,
 941 2005; Widmann et al., 2019; McKanna et al., 2023). This is clearly observed for the treated and untreated aliquots of
 942 igneous sample MIGU-02, where the treated aliquot has substantially lower ^{238}U beam intensities and increased
 943 concordance and accuracy in $^{206}\text{Pb}/^{238}\text{U}$ dates (Figs. 3, 4, and 5). However, the thermal history is not known *a priori*
 944 for detrital zircon datasets, meaning this same assessment applied to NM8A and Rora Med is more uncertain.

945 To examine whether the reduced Pb-loss we observed in the chemically abraded aliquot reflects the selective
 946 dissolution of zircon with radiation damage, we compared zircon ^{238}U beam intensity from a particular age range (250-
 947 320 Ma) in NM8A as a first-order approximation (Fig. 9). We assume that the populations in this range likely have
 948 the same low-T history, although this assumption cannot be tested with our data. We also note that these populations
 949 showed the most significant sharpening following chemical abrasion (Fig. 7B). Figure 9 shows that the average ^{238}U
 950 beam intensity of treated grains in this age range is similar, but there is a distinct proportion of treated grains that have
 951 lower ^{238}U intensities. This supports our interpretation that CA is likely mitigating Pb-loss by dissolving zircon with
 952 high U concentrations and that this process can be observed by the changes in the number of peaks, their shape, and
 953 their magnitude between treated and untreated aliquots. These changes are especially apparent when comparing the
 954 shift and change in magnitude of the Rora Med 2665-2685 Ma (untreated aliquot) peak age to 2690-2715 Ma (treated
 955 aliquot).



956 **Figure 9.** Histogram showing ^{238}U cps (normalized to SL) for zircons in the peak age population between 250-320 Ma in detrital zircon sample NM8A. On the detrital zircon spectra, this age population narrows from one broad peak in the untreated aliquot to a well-defined, narrow

964 peak in the treated aliquot (Fig. 7b). Measured ^{238}U cps from this peak age population of treated and untreated aliquots
 965 are overall similar, but there is a distinguishable proportion of grains in the treated aliquot that have lower ^{238}U cps.

967 Reduced Pb-loss in Mesoproterozoic and older zircon also benefits detrital zircon studies because ancient
 968 Pb-loss can bias $^{207}\text{Pb}/^{206}\text{Pb}$ dates of moderately discordant or even (analytically) concordant zircon toward
 969 erroneously young values (Nemchin and Cawood, 2005). This effect has led many laboratories to filter for discordance
 970 within their datasets. Thus, improving concordance will increase the proportion of dates that can be retained in a
 971 detrital zircon study and improve confidence in the identification of peak age populations. One potential issue with
 972 this approach is the possibility that entire zircon populations could be removed during chemical abrasion if they have
 973 high degrees of radiation damage. Surprisingly, we did not see this effect in either NM8A nor Rora Med. This result
 974 is surprising and may be sample specific, since Rora Med zircon from all age populations have low ^{238}U beam
 975 intensities (Fig. 10b). Although our RoraMed sample did not entirely lose any age populations during CA, changes in

- Deleted: U concentrations
- Deleted: cps...eam intensities and increased concordance and accuracy of measured (... [6])
- Deleted: 2... 43... and 54 (... [7])
- Deleted: concentrations
- Deleted: cps...eam intensity from a particular age range (250-320 Ma) in NM8A as a first-order approximation (Fig. 9). We assume that the populations in this range likely have the same low-T cooling ... history, although with the caveat that ...his assumption remains unknown and (... [8])
- Formatted: Superscript
- Deleted: 6...). Figure 98...shows that the average ^{238}U concentration (... [9])
- Deleted: cps...eam intensity of treated grains in this age range is similar, but there is a distinguishable (... [10])
- Deleted: cps
- Deleted: and indistinguishable to the untreated aliquot, indicating that we cannot determine if
- Formatted: Superscript
- Deleted: these...hat this process effects ...an be observed by the changes in the number of peaks, peak...heir shape, and peak...heir magnitude between treated and untreated aliquots. These changes is ...reis (... [11])
- Deleted: chemical abrasion selectively removed analyses that had Pb-loss.
- Deleted: Note, however, that due to the unknown thermal history of the detrital zircon in this sample and sample NM8A itself, it is much more difficult to directly compare ^{238}U c concentrations between detrital zircon aliquots than it is between igneous zircon from the same unit (e.g., MIGU-02) since we cannot assume that all zircons of the same age have experience the same thermal history. However, our limited datasets do suggest that overall reduced ^{238}U cps in treated aliquots of both Rora Med and NM8A reflect CA mitigating zones of higher U, commonly associated with Pb-loss.
- Deleted: 8
- Deleted: concentration (ppm)
- Formatted: Superscript
- Deleted: 6
- Deleted: concentrations
- Formatted: Superscript
- Deleted: and indistinguishable... (... [12])
- Formatted: Superscript
- Deleted: will
- Deleted: concentrations
- Deleted: cps
- Formatted: Superscript
- Deleted: (<500 ppm;... .ig. 109...). Although our (... [13])

1079 the magnitude of peak heights suggests preferential dissolution of some age populations associated with Pb-loss. This
 1080 feature may be unique to Precambrian samples with overall low zircon U concentrations and/or recent exhumation of
 1081 the sedimentary rocks to the temperature conditions where radiation damage can accumulate and Pb-loss occurs.
 1082 Regardless, both NM8A and Rora Med have similarity values of >0.9 (Figs. 6 and &), indicating that similar peak age
 1083 populations and proportions are present in both treated and untreated aliquots. Therefore, it is unlikely that chemical
 1084 abrasion would impact detrital zircon spectra in a way that would make aliquots look as though they were sampling
 1085 different source terranes.

Deleted: partial
 Deleted: t
 Deleted: low
 Deleted: from different samples or sourcing

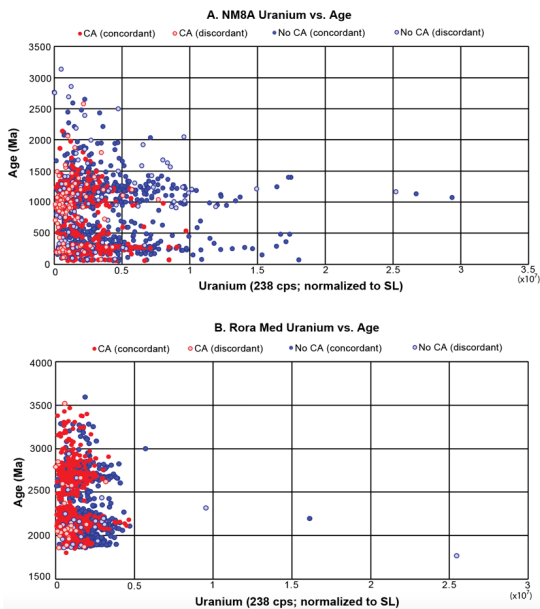


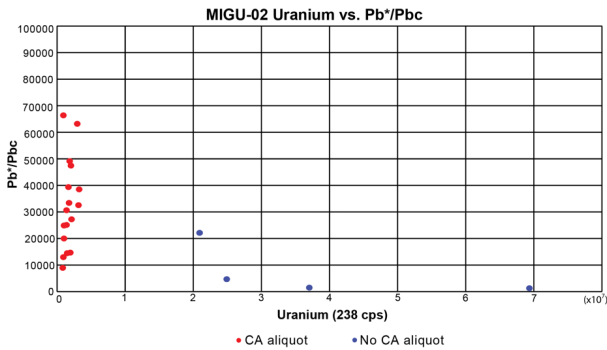
Figure 10. Scatter plot of ^{238}U cps (normalized to SL) plotted against the age (Ma) for both treated and untreated aliquots of A. NM8A and B. Rora Med. Both concordant and discordant analyses are shown. Overall, CA appears effectively reduce scatter in ^{238}U cps in all age populations compared to the untreated aliquot, but most significantly reduces scatter in Precambrian ages.

Deleted: ¶
 Deleted: 9
 Deleted: uranium concentrations (ppm)
 Formatted: Superscript
 Deleted: to
 Deleted: the
 Deleted: in U concentrations for
 Deleted: ages compared to the untreated aliquot in NM8A. Overall, all analyzed zircons in treated and untreated aliquots of Rora Med have low U concentrations (<500 ppm), and therefore minor differences in U concentrations are seen between treated and untreated aliquots.

1105 The nature of sediment transport may also work to remove metamict zircon prior to deposition in certain
 1106 environments. Hydraulic sorting, mechanical abrasion, and weathering, can naturally bias detrital zircon populations
 1107 present in a different lithologies (Malusa et al., 2013; Ibañez-Mejia et al., 2018). For example, Ewing et al. (2003)
 1108 noted that metamictization leads to structural damage of the zircon crystal structure and that this can be correlated to
 1109 a decrease in density and hardness. These changes lead metamict zircon to be more prone to destruction during river
 1110 transport (Fedot et al., 2003; Hay and Dempster, 2009a). In particular, Hay and Dempster (2009a) argue that inclusion-
 1111 rich and metamict zircon are broken during sediment transport, and that these fragments do not survive being
 1112 incorporated into clastic sandstone deposits. Instead, these smaller fragments can be swept out to more distal
 1113 depositional environments. Small zircon are also typically lost during sample preparation (Hietpas et al., 2011; Slama
 1114 and Kosler, 2012), meaning that both natural and laboratory processes may preferentially lead to a high proportion of
 1115 undamaged zircon in sandstone samples. Thus, while we did not observe the removal of specific age populations

1131 following chemical abrasion in the two detrital zircon samples that were analyzed in this study, and there are reasons
 1132 to suspect that natural and laboratory processes will favor the analysis of undamaged zircon anyway, we recognize
 1133 that other samples may behave differently. Future users of this technique should carefully consider this possibility in
 1134 their datasets.

1135 Another potential benefit of chemical abrasion is the preferential dissolution of inclusions within zircon
 1136 during the partial dissolution step (McKanna et al., 2023). Inclusions harbor Pb_c that can be incorporated into the
 1137 analyzed volume during laser ablation, reducing the Pb*/Pbc and limiting measurement precision and accuracy. When
 1138 comparing the Pb*/Pbc ratios of treated and untreated aliquots of MIGU-02, we see a clear distinction that treated
 1139 zircons have a much higher Pb*/Pbc ratio for similar ranges in ²³⁸U beam intensity (Fig. 11). We note that the overall
 1140 ²³⁸U beam intensities for the treated aliquot of MIGU-02 are low compared to the untreated aliquot, as we have already
 1141 shown that CA for metamict zircon effectively removes high-U zones where Pb-loss is most likely to have occurred
 1142 (see above discussion; Fig. 5). Regardless, the increased Pb*/Pbc ratio for the treated aliquot of MIGU-02 shows that
 1143 this method is also efficient in removing inclusions with high Pb_c content and/or highly damaged domains where Pb_c
 1144 might have been introduced by fluids. These two effects are correlated with an increased fraction of concordant grains
 1145 and increased precision and accuracy in ²⁰⁶Pb/²³⁸U zircon dates in the chemically abraded aliquot. These observations
 1146 support the benefits of utilizing CA prior to LA-ICP-MS measurements in metamict igneous zircon suites. A
 1147 comparison of the Pb*/Pbc ratios in treated and untreated aliquots of detrital samples (Fig. S18) shows similar behavior
 1148 in Rora Med with slightly higher Pb*/Pbc in the treated aliquot and no change in the Pb*/Pbc ratios in NM8A. We
 1149 conclude that it is likely that CA is removing inclusions prior to analysis of detrital zircons as well. However, it is
 1150 difficult to isolate this effect since detrital zircons are sourced from various terranes and we cannot confidently
 1151 compare the Pb*/Pbc of zircon with the same age, U concentration, and thermal history.



1152 **Figure 11**, Pb*/Pbc ratios are plotted against ²³⁸U cps for MIGU-02. The Pb*/Pbc ratios in the treated aliquot of MIGU-02 are significantly higher than the untreated aliquot for similar concentrations of U. Higher Pb*/Pbc ratios in the treated aliquot of MIGU-02 can be attributed to reduction of Pb_c by removal of inclusions.

1163
 1164 **6. Conclusions and Recommended Applications**
 1165 Chemical abrasion is a widely used tool in the zircon U-Pb ID-TIMS community (see reviews in Schoene,
 1166 2014; Schaltegger et al., 2015), where it has been repeatedly shown to mitigate the negative effects on age accuracy
 1167 introduced by Pb-loss (Mundil et al., 2004; Mattinson, 2005; Widmann et al., 2019). Recent efforts to extend chemical
 1168 abrasion to LA-ICP-MS analyses have also shown that this pre-treatment can be beneficial (Crowley et al., 2014; Von

- Deleted: U concentration
- Deleted: cps
- Deleted: 0
- Deleted: concentrations
- Deleted: cps
- Formatted: Superscript
- Deleted: 4
- Deleted: percent
- Deleted: ce
- Deleted: ,
- Deleted: ,
- Deleted: observed
- Deleted: of the treated aliquot of MIGU-02
- Deleted: ,
- Moved down [2]: It is likely that this same effect occurs in detrital zircons suites that are treated by chemical abrasion.
- Deleted: ing
- Deleted: When
- Deleted: comparing
- Deleted: of
- Deleted: Rora Med
- Deleted: ,
- Deleted: overall the ratios are
- Formatted: Subscript
- Moved (insertion) [2]
- Deleted: , but we see slightly higher ratios in the treated aliquot of Rora Med. The Pb*/Pbc ratios remain indistinguishable and strongly overlap when comparing treated and untreated aliquots of NM8A (Fig. SX). It is likely that this same effect of increasing Pb*/Pbc ratios occurs in detrital zircons suites that are treated by chemical abrasion. Although
- Deleted: <object>
- Deleted: 0
- Deleted: uranium
- Deleted: 5

1202 Quadt et al., 2014; McKanna et al., 2023; Sharman and Malkowski, 2023). The extension of this pre-treatment to
1203 large-n detrital zircon analyses is a natural outgrowth of these efforts. Our results indicate no negative effects from
1204 chemical abrasion prior to LA-ICP-MS analyses and that the technique results in improved percentages of concordant
1205 grains, reduced uncertainty, and, at least for the highly radiation damaged igneous sample we studied here, accuracy
1206 of measured U-Pb dates. For DZ samples, these benefits appear to translate to more defined and slightly older
1207 ²⁰⁶Pb/²³⁸U age peaks for Phanerozoic zircon, and more concordant analyses, and in some cases slightly older
1208 ²⁰⁷Pb/²⁰⁶Pb dates, for Precambrian zircon. One potential drawback of this pre-treatment is the possibility that age
1209 populations characterized by high-U zircon may be selectively dissolved during chemical abrasion. We did not observe
1210 this effect in either of our tested samples. However, we remain wary of its possibility in other samples with highly
1211 damaged Precambrian zircon populations, and so future practitioners are advised caution. The differences between
1212 age distributions in our analyzed detrital zircon spectra are slight and indicate that the Pb-loss present in typical
1213 untreated analyses would not significantly alter the interpretation of sediment source terranes at a broad scale.
1214 However, chemical abrasion did sharpen several Phanerozoic peak ages and led to an increased percentage of
1215 concordant grains in Precambrian zircon populations. This indicates that the pre-treatment may be useful in certain
1216 scenarios in which researchers may require increased resolution of detrital zircon age spectra to distinguish fine-scale
1217 variations in provenance, sediment source terranes, or source characteristics. Ongoing research aims to test this
1218 method's impact on improving the precision and accuracy of maximum depositional age (MDA) estimations.

Deleted: concordance

Deleted: precision

Deleted: ,

Deleted: ce

Deleted: ,

Deleted: ing

1220 Supplement

1221 All datasets utilized in this study are available in the Supplementary Materia online at:

1223 Author contribution

1224 EED, MPE, and MIM all helped design experiments for treated and untreated zircon aliquots and EED prepared all
1225 bulk chemically abraded aliquots and conducted CA-ID-TIMS experiments. FM and EED both conducted LA-ICP-
1226 MS and CA-LA-ICP-MS experiments. FM and MIM designed and FM conducted zircon optical profilometry
1227 experiments. All authors participated in the interpretation and discussion of results. EED prepared the figures and
1228 manuscript.

Deleted: and

Deleted: ed

Deleted: conducted

Deleted: the

Deleted:

1230 Competing Interests

1231 The authors declare no competing interests.

1233 Acknowledgments

1234 We thank the Arizona LaserChron Center (ALC) for sharing samples and reference materials and for helping
1235 analyze these samples. Specifically, we thank G. Gehrels, M. Pecha, D. Alberts, W. Allen, M. Foley, and T. Milster.
1236 We also thank R. Ickert for help designing a system for bulk CA at Purdue. All LA-ICPMS measurements were
1237 made at the Arizona LaserChron Center under NSF-EAR 2050246 for support of the Arizona LaserChron Center
1238 and all CA steps and CA-ID-TIMS measurements were completed at Purdue University's Radiogenic Isotope
1239 Geology Lab (RIGL) under NSF-EAR-2151277 to M. Eddy.

Deleted: and

1252

1253

References

1254

Anderson, T.: Detrital zircons as tracers of sedimentary provenance: limiting conditions from statistics and numerical simulation, *Chemical Geology*, 216, 249–270, doi: <https://doi.org/10.1016/j.chemgeo.2004.11.013>, 2005.

1255

1256

Balan, E., Neuville, D.R., Trocellier, P., Fritsch, E., Muller, J. P., Calas, G.: Metamictization and chemical durability of detrital zircon, *Am. Mineral.*, 86, 1025-1033, 2001.

1258

1259

Bateman, H.: Solution of a system of differential equations occurring in the theory of radioactive transformations, *Proceedings of the Cambridge Philosophical Society*, 15, 423-427, 1910.

1260

1261

Black, L.P.: Recent Pb loss in zircon: a natural or laboratory-induced phenomenon?, *Chemical Geology*, 65 25-33, 1987.

1262

1263

Black, L.P., Kamo, S.L., Allen, C.M., Alcinikoff, J.N., Davis, D.W., Korsch, R.J., and Foudoulis, C.: TEMORA-1: A new zircon standard for Phanerozoic U-Pb geochronology, *Chemical Geology*, 200, 155-170, 2003.

1266

1267

1268

Black, L.P., Kamo, S.L., Allen, C.M., Davis, D.W., Alcinikoff, J.N., Valley, J.W., Mundil, R., Campbell, I.H., Korsch, R.J., Williams, I.S., and Foudoulis, C.: Improved ²⁰⁶Pb/²³⁵U microprobe geochronology by the monitoring of a trace-element-related matrix effect; SHRIMP, ID-TIMS, ELA-ICP-MS and oxygen isotope documentation for a series of zircon standards, *Chemical Geology*, 205, 115-140, doi:

1271

<https://doi.org/10.1016/j.chemgeo.2004.01.003>, 2004

1272

1273

Bowring, J.F., McLean, N.M., and Bowring, S.A.: Engineering cyber infrastructure for U-Pb geochronology: Tripoli and U-Pb redux, *Geochemistry, Geophysics, and Geosystems*, 12, doi: <https://doi.org/10.1029/2010GC003479>, 2011

1274

1275

Carrapa, B., 2010: Resolving tectonic problems by dating detrital minerals, *Geology*, 38, 191–92, doi: <https://doi.org/10.1130/focus022010.1>, 2010

1276

1277

Chakoumakos, B.C., Murakami, T., Lumpkin, G.R., and Ewing, R.C.: Alpha-decay induced fracturing in zircon: The transition from the crystalline to metamict state, *Science*, 236, 1556-1559, 1987.

1281

1282

Condon, D.J., Schoene, B., McLean, N.M., Bowring, S.A., and Parrish, R.R.: Metrology and traceability of U-Pb isotopic dilution geochronology (EARTHTIME tracer calibration part 1), *Geochimica et Cosmochimica Acta*, 164, 464-480, 2015

1284

1285

Coutts, D.S., Matthews, W.A., and Hubbard, S.M.: Assessment of widely used methods to derive depositional ages from detrital zircon populations, *Geoscience Frontiers*, 10, 1421-1435, 2019.

1286

1287

Crowley J.L., Schoene, B., and Bowring, S.A: U–Pb dating of zircon in the Bishop Tuff at the millennial scale, *Geology*, 35, 1123–1126, doi: <https://doi.org/10.1130/G24017A.1>, 2007

1291

1292

Crowley, Q.G., Heron, K., Riggs, N., Kamber, B., Chew, D., McConnell, B., and Benn, K.: Chemical Abrasion Applied to LA-ICP-MS U-Pb Zircon Geochronology, *Minerals*, 4, 503-518, doi: <https://doi.org/10.3390/min4020503>, 2014

1296

1297

Dickin, A.P.: Radiogenic Isotope Geology, 2nd Ed., Cambridge, UK: Cambridge University Press, 2005.

1298

1299

Dickinson, W.R., and Gehrels, G.E.: Use of U-Pb ages of detrital zircons to infer maximum depositional ages of strata: a test against a Colorado Plateau Mesozoic database, *Earth and Planetary Science Letters*, 288, 115-125, 2009.

1300

1301

Eddy, M.P., Ibañez-Mejía, M., Burgess, S.D., Coble, M.A., Cordani, U.G., DesOrmeau, J., Gehrels, G.E., Li, X., MacLennan, S., Pecha, M., Sato, K., Schoene, B., Valencia, V.A., Vervoort, J.D., and Wang, T.: GHR1 Zircon – A

1302

1303

1304

1305

Formatted: Superscript

1306 New Eocene Natural Reference Material for Microbeam U-Pb Geochronology and Hf Isotopic Analysis of Zircon,
1307 *Geostandards and Geoanalytical Research*, 43, 113-132, doi: <https://doi.org/10.1111/ggr.12246>, 2019.

1308

1309 Ewing, R.C., Meldrum, A., Wang, L., Weber, W.J., Corrales, I.R.: Radiation effects in zircon *In* Hanchar, J.M.,
1310 Hoskin, P.W.O. (Eds.), *Zircon. Rev. Mineral. Geochem.*, 53, *Mineral Society of America*, 277-303, 2003.

1311

1312 Fedo C.M., Sircombe, K., and Rainbird, R.: Detrital zircon analysis of the sedimentary record, *Reviews in
1313 Mineralogy and Geochemistry*, 53, 277-303, doi: <https://doi.org/10.2113/0530277>, 2003

1314

1315 [Garver, J.I., and Kamp, P.J.J.: Integration of zircon color and zircon fission track zonation patterns in orogenic belts:
1316 Application of Southern Alps, New Zealand, *Tectonophysics*, 349, 203-219, 2002.](#)

1317

1318 Gehrels, G.E.: Detrital zircon U-Pb geochronology: current methods and new opportunities, *In Tectonics of
1319 Sedimentary Basins: Recent Advances*, eds C., Busby, A., Azor, pp. 47–62, Chichester, UK: Wiley-Blackwell, 2012

1320

1321 Gehrels, G.E., Valencia, V., Ruiz, J.: Enhanced precision, accuracy, efficiency, and spatial resolution of U-Pb ages
1322 by laser ablation–multicollector–inductively coupled plasma–mass spectrometry, *Geochemistry, Geophysics, and
1323 Geosystems*, 9, doi: <https://doi.org/10.1029/2007GC001805>, 2008

1324

1325 Gehrels, G.E.: Detrital zircon U-Pb Geochronology Applied to Tectonics: *Annual Review of Earth and Planetary
1326 Sciences*, 42, 127-149, doi: <https://doi.org/10.1146/annurev-earth-050212-124012>, 2014

1327

1328 Gehrels, G.E., and Pecha, M.: Detrital zircon U-Pb geochronology and Hf isotope geochemistry of Paleozoic and
1329 Triassic passive margin strata of western North America, *Geosphere*, 10, 49–65, doi:
1330 <https://doi.org/10.1130/GES00889.1>, 2014

1331

1332 Gehrels, G.E., Valencia, V., Pullen, A.: Detrital zircon U-Pb geochronology by Laser-Ablation Multicollector
1333 ICPMS at the Arizona LaserChron Center, in Loszewski, T., and Huff, W., eds., *Geochronology: Emerging
1334 Opportunities*, Paleontology Society Short Course: Paleontology Society Papers, 11, 2006.

1335

1336 [Ginster, U., Reiners, P.W., Nasdala, L., and Chanmuang C.N.: Annealing kinetics of radiation damage in zircon,
1337 *Geochimica et Cosmochimica Acta*, 15, 225-246, 2019.](#)

1338

1339 [Goldich, S.S., and Mudrey, Jr., M.G.: Dilatancy model for discordant U-Pb zircon ages. In: A.I. Tugarinov \(ed\),
1340 *Contributions to Recent Geochemistry and Analytical Chemistry \(Vinogradov Volume\)*, 415-418, 1972.](#)

1341

1342 [Herriot, T.M., Crowley, J.L., Schmitz, M.D., Marwan, W.A., and Gillis, R.J.: Exploring the law of detrital zircon:
1343 LA-ICP-MS and CA-TIMS geochronology of Jurassic forearc strata, Cook Inlet, Alaska, USA, *Geology*, 47, 1044-
1344 1048: <https://doi.org/10.1130/G46312.1>, 2019](#)

1345

1346 Hay, D.C., and Dempster, T.J.: Zircon alteration, formation, and preservation in sandstones, *Sedimentology*, 56,
1347 2175-2191, doi: 10.1111/j.1365-3091.2009.01075.x, 2009.

1348

1349 Hay, D.C., and Dempster, T.J.: Zircon behaviour during low temperature metamorphism, *Journal of Petrology*, 50,
1350 571-598, 2009.

1351

1352 Hiess, J., Condon, D. J., McLean, N. and Noble, S. R.: 238U/235U Systematics in Terrestrial Uranium-Bearing
1353 Minerals, *Science*, 335, 1610–1614, 2012

1354

1355 Hietpas, J., Samson, S., Moecher, D., Chakraborty, S.: Enhancing tectonic and provenance information from detrital
1356 zircon studies: assessing terrane-scale sampling and grain-scale characterization, *J. Geol. Soc. Lond.*, 168, 309-318,
1357 2011.

1358

1359 Ibañez-Mejía, M., Pullen, A., Pepper, M., Urbani, F., Ghoshal, G., and Ibañez-Mejía, J.C.: Use and abuse of detrital
1360 zircon U-Pb geochronology – A case from the Rio Orinoco delta, eastern Venezuela, *Geology*, 46, 1019-1022, 2018.

1361

1362 Jaffey, A.H., Flynn, K.F., Glendenin, L.E., Bentley, W.C., and Essling, A.M.: Precision Measurement of Half-Life
1363 and Specific Activities of ²³⁵U and ²³⁸U, *Physical Review C*, 4, 1971.
1364
1365 [Keller, C.B., Boehnke, P., Schoene, B., and Harrison, M.: Stepwise chemical abrasion-isotope dilution-thermal
1366 ionization mass spectrometry with trace element analysis of microfractured Hadean zircon, *Geochronology*, 1, 85-
1367 97, 2019.](#)
1368
1369 [Kramers, J., Frei, R., Newville, M., Kober, B., Villa, I.: On the valency state of radiogenic lead in zircon and its
1370 consequences, 261, 4-11, 2009.](#)
1371
1372 Malusa, M.G., Carter, A., Limoncelli, M., Villa, I. M., and Garzanti, E.: Bias in detrital zircon geochronology and
1373 thermochronometry, *Chemical Geology*, 359, 90-107, 2013.
1374
1375 [Marsellos, A.E., and Garver, J.J.: Radiation damage and uranium concentration in zircon as assessed by Raman
1376 spectroscopy and neutron irradiation, *American Mineralogist*, 95, p. 1192-1201, 2010.](#)
1377
1378 [Mattinson, J.M.: A study of complex discordance in zircons using step-wise dissolution techniques, *Contributions to
1379 Mineralogy and Petrology*, 116, 117-129, 1994.](#)
1380
1381 Mattinson J.M.: Zircon U–Pb chemical-abrasion ("CA-TIMS") method: Combined annealing and multi-step
1382 dissolution analysis for improved precision and accuracy of zircon ages, *Chemical Geology*, 220, 47–56, doi:
1383 <https://doi.org/10.1016/j.chemgeo.2005.03.011>, 2005
1384
1385 Mattinson, J.M.: Analysis of the relative decay constants of ²³⁵U and ²³⁸U by multi-step CA-TIMS measurements
1386 of closed system natural zircon samples, *Chemical Geology*, 275, 186-198, doi:
1387 <https://doi.org/10.1016/j.chemgeo.2010.05.007>, 2010
1388
1389 McConnell, B., Riggs, N., and Crowley, Q.G.: Detrital zircon provenance and Ordovician terrane amalgamation,
1390 western Ireland, *Journal of the Geological Society*, 166, 473–484, doi: <https://doi.org/10.1144/0016-76492008-081>,
1391 2009
1392
1393 McKanna, A.J., Koran, I., Schoene, B., and Ketcham, R.A.: Chemical abrasion: the mechanics of zircon dissolution,
1394 *Geochronology*, 5, 127-151, <https://doi.org/10.5194/gchron-5-127-2023>, 2023
1395
1396 McLean, N.M., Condon, D.J., Schoene, B., and Bowring, S.A.: Evaluating uncertainties in the calibration of isotopic
1397 reference materials and multi-element isotopic tracers (EARTHTIME tracer calibration II), *Geochimica et
1398 Cosmochimica Acta*, 164, 481-501., 2015
1399
1400 Mundil, R., Ludwig, K.R., Metcalfe, I., and Renne, P.R.: Age and timing of the Permian mass extinctions: U/Pb
1401 dating of closed-system zircons, *Science*, doi: 10.1126/science.1101012., 2004
1402
1403 [Nasdala, L., Hanchar, J.M., Kronz, A., Whitehouse, M.J.: Long-term stability of alpha particle damage in natural
1404 zircon, *Chemical Geology*, 220, 83-103, doi: <https://doi.org/10.1016/j.chemgeo.2005.03.012>, 2005](#)
1405
1406 Nemchin, A., and Cawood, P.: Discordance of the U-Pb system in detrital zircons: Implication for provenance
1407 studies of sedimentary rocks, *Sediment Geol.*, **182**, 143–162, 2005
1408
1409 Parrish, R.R., and Noble, S.R.: Zircon U–Th–Pb geochronology by isotope dilution –Thermal ionization mass
1410 spectrometry (ID-TIMS): In Hanchar JM and Hoskin PWO (eds.) *Zircon, Reviews in Mineralogy and Geochemistry*,
1411 53, 183–213, Washington, DC: Mineralogical Society of America, 2003
1412
1413 Pullen., A., Ibañez-Mejia, M., Gehrels, G.E., Ibanez-Mejia, J.C., and Pecha, M.: What happens when n=1000?
1414 Creating large-n geochronological datasets with LA-ICP-MS for geologic investigations, *Journal of Analytical
1415 Spectrometry*, 6, doi: <https://doi.org/10.1039/C4JA00024B>., 2014
1416

Deleted: ¶

Deleted: ¶

1419 Pullen, A., Ibañez-Mejía, M., Gehrels, G.E., Giesler, D., and Pecha, M.: Optimization of a Laser Ablation-Single
1420 Collector-Inductively Coupled Plasma-Mass Spectrometer (Thermo Element 2) for Accurate, Precise, and Efficient
1421 Zircon U-Th-Pb Geochronology, *Geochemistry, Geophysics, and Geosystems*, 19, 3689-3705, 2018.
1422
1423 Rahn, M.K., Brandon, M.T., Batt, G.E., Garver, J.I.: A zero damage model for fission-track annealing in zircon, *Am.
1424 Mineral*, 89, 473-484, 2004.
1425
1426 [Reiners, P.W.: Zircon \(U-Th\)/He Thermochronometry, *Reviews in Mineralogy & Geochemistry*, 58, 151-179, 2005.](#)
1427
1428 [Satkoski, A.M., Wilkinson, B.H., Hietpas, J., and Samson, S.D.: Likeness among detrital zircon populations – An
1429 approach to the comparison of age frequency data in time and space, *Geological Society of America Bulletin*, 125,
1430 1783-1799, 2013.](#)
1431
1432 [Saylor, J.E., and Sundell, K.E.: Quantifying comparison of large detrital geochronology data sets, *Geosphere*, 12, 1-
1433 18, 2016.](#)
1434
1435 Schaltegger, U., Schmitt, A.K., and Horstwood, M.S.A.: U-Th-Pb zircon geochronology by ID-TIMS, SIMS, and
1436 laser ablation ICP-MS: recipes, interpretations, and opportunities, *Chem. Geol.*, 402, 89-110,
1437 <https://doi.org/10.1016/j.chemgeo.2015.02.028>, 2015
1438
1439 Schmitz, M.D., and Bowring, S.A.: U-Pb zircon and titanite systematics of the Fish Canyon Tuff: an assessment of
1440 high-precision U-Pb geochronology and its application to young volcanic rocks, *Geochimica et Cosmochimica Acta*,
1441 65, 2571-2587, 2001
1442
1443 Schoene, B.: U-Th-Pb Geochronology, Treatise on geochemistry 2nd edition, doi: [http://dx.doi.org/10.1016/B978-0-
1444 08-095975-7.00310-7](http://dx.doi.org/10.1016/B978-0-08-095975-7.00310-7), 2014
1445
1446 [Sharman, G.R., and Malkowski, M.A.: Needles in a haystack: Detrital zircon U-Pb ages and the maximum
1447 depositional age of modern global sediment, *Earth Science Reviews*, 203, 2020](#)
1448
1449 Smith, T.M., Saylor, J.E., Lapen, T.J., Leary, R.J., and Sundell, K.E.: Large detrital zircon data set investigation and
1450 provenance mapping: Local versus regional and continental sediment sources before, during, and after Ancestral
1451 Rocky Mountain deformation, *GSA Bulletin*, doi: <https://doi.org/10.1130/B36285.1>, 2023
1452
1453 Sláma, J., Kosler, J., Condon, D.J., Crowley, J.L., Gerdes, A., Hanchar, J.M., Horstwood, M.S.A., Morris, G.A.,
1454 Nasdala, L., Norberg, N., Schaltegger, U., Schoene, B., Tubrett, M.N., and Whitehouse, M.J.: Plesovice zircon – A
1455 new natural reference material for U-Pb and Hf isotopic microanalysis, *Chemical Geology*, 249, 1-35, doi:
1456 <https://doi.org/10.1016/j.chemgeo.2007.11.005>, 2008
1457
1458 Slama, J., and Kosler, J.: Effects of sampling and mineral separation on accuracy of detrital zircon studies,
1459 *Geochemistry, Geophysics, Geosystems*, 13, 2012.
1460
1461 [Stern, R.A., Bodorkos, S., Kama, S.L., Hickman, A.H., and Corfu, F.: Measurement of SIMS instrumental mass
1462 fractionation of Pb isotopes during zircon dating, *Geostandards and Geoanalytical Research*, 33, 145-168, doi:
1463 <https://doi.org/10.1111/j.1751-908X.2009.00023.x>, 2009
1464
1465 Sundell, K. E., Gehrels, G. E., and Pecha, M. E.: Rapid U-Pb Geochronology by Laser Ablation Multi-Collector
1466 ICP-MS, *Geostand Geoanal Res.*, 45, 37–57, 2021
1467
1468 \[Vermeesch, P.: Maximum depositional age estimation revisited, *Geoscience Frontiers*, 12, 843-850, 2021.\]\(#\)
1469
1470 Von Quadt, A., Dallhofer, D., Guilong, M., Peytcheva, I., Waelle, M., and Sakata, S.: U-Pb dating of CA/non-CA
1471 treated zircons obtained by LA-ICP-MS and CA-TIMS techniques: impact for their geological interpretation,
1472 *Journal of Analytical Atomic Spectrometry*, 29, 1618-1629, doi: <https://doi.org/10.1039/C4JA00102H>, 2014
1473](#)

Deleted: ¶

1475 Wang, J. W., Gehrels, G., Kapp, P. & Sundell, K.: Evidence for regionally continuous Early Cretaceous sinistral
1476 shear zones along the western flank of the Coast Mountains, coastal British Columbia, Canada, *Geosphere*, 19, 139–
1477 162, 2022.

1478

1479 Widmann, P., Davies, J.H.F.L., and Schaltegger, U.: Calibrating chemical abrasion: Its effects on zircon crystal
1480 structure, chemical composition and U-Pb age. *Chemical Geology*, 511, 1-10,
1481 <https://doi.org/10.1016/j.chemgeo.2019.02.026>, 2019.

1482

1483 Wiedenbeck, M., Alle, P., Corfu, F., Griffin, W.L., Meier, M., Oberli, F., von Quadt, A., Roddick, J.C., and Spiegel,
1484 W.: Three natural zircon standards for U-Th-Pb, Lu-Hf, trace element and REE analyses, *Geostandards Newsletter*,
1485 v. 19, p. 1-23, 1995

1486

1487 Wiedenbeck, M., Hanchar, J.M., Peck, W.H., Sylvester, P., Valley, J., Whitehouse, M., Kronz, A., Morishita, Y.,
1488 Nasdala, L., Fiebig, J., Franchi, I., Girard, J.P., Greenwood, R.C., Hinton, R., Kita, N., Mason, P.R.D., Norman, M.,
1489 Ogasawara, M., Piccoli, P.M., Rhede, D., Satoh, H., Schultz-Dobrick, B., Skar, O., Spicuzza, M.J., Terada, K.,
1490 Tindle, A., Togashi, S., Vennemann, T., Xie, Q., and Zheng, Y.F.: Further characterization of the 91500 zircon
1491 crystal, *Geostandards and Geoanalytical Research*, v. 28, p. 9-39, doi: [https://doi.org/10.1111/j.1751-](https://doi.org/10.1111/j.1751-908X.2004.tb01041.x)
1492 [908X.2004.tb01041.x](https://doi.org/10.1111/j.1751-908X.2004.tb01041.x), 2004

1493

1494 Wotzlaw, J.F., Schaltegger, U., Frick, D.A., Dungan, M.A., Gerdes, A., and Gunther, D.: Tracking the evolution of
1495 large-volume silicic magma reservoirs from assembly to supereruption, *Geology*, 41, 867-870, 2013

1496

Moved (insertion) [1]

Deleted: ¶

Field Code Changed

Moved up [1]: Widmann, P., Davies, J.H.F.L., and Schaltegger, U.: Calibrating chemical abrasion: Its effects on zircon crystal structure, chemical composition and U-Pb age, *Chemical Geology*, 511, 1-10, <https://doi.org/10.1016/j.chemgeo.2019.02.026>, 2019¶

Deleted: ¶

Page 12: [1] Deleted Donaghy, Erin Elizabeth 11/2/23 1:50:00 PM

Page 12: [1] Deleted Donaghy, Erin Elizabeth 11/2/23 1:50:00 PM

Page 12: [1] Deleted Donaghy, Erin Elizabeth 11/2/23 1:50:00 PM

Page 12: [1] Deleted Donaghy, Erin Elizabeth 11/2/23 1:50:00 PM

Page 12: [1] Deleted Donaghy, Erin Elizabeth 11/2/23 1:50:00 PM

Page 12: [1] Deleted Donaghy, Erin Elizabeth 11/2/23 1:50:00 PM

Page 12: [1] Deleted Donaghy, Erin Elizabeth 11/2/23 1:50:00 PM

Page 12: [1] Deleted Donaghy, Erin Elizabeth 11/2/23 1:50:00 PM

Page 12: [1] Deleted Donaghy, Erin Elizabeth 11/2/23 1:50:00 PM

Page 12: [1] Deleted Donaghy, Erin Elizabeth 11/2/23 1:50:00 PM

Page 12: [1] Deleted Donaghy, Erin Elizabeth 11/2/23 1:50:00 PM

Page 12: [1] Deleted Donaghy, Erin Elizabeth 11/2/23 1:50:00 PM

Page 12: [1] Deleted Donaghy, Erin Elizabeth 11/2/23 1:50:00 PM

Page 12: [1] Deleted Donaghy, Erin Elizabeth 11/2/23 1:50:00 PM

Page 12: [1] Deleted Donaghy, Erin Elizabeth 11/2/23 1:50:00 PM

Page 12: [1] Deleted Donaghy, Erin Elizabeth 11/2/23 1:50:00 PM

Page 12: [1] Deleted Donaghy, Erin Elizabeth 11/2/23 1:50:00 PM

Page 12: [1] Deleted Donaghy, Erin Elizabeth 11/2/23 1:50:00 PM

Page 12: [1] Deleted Donaghy, Erin Elizabeth 11/2/23 1:50:00 PM

Page 12: [1] Deleted Donaghy, Erin Elizabeth 11/2/23 1:50:00 PM

Page 12: [2] Deleted Donaghy, Erin Elizabeth 1/17/24 7:07:00 PM

Page 12: [2] Deleted Donaghy, Erin Elizabeth 1/17/24 7:07:00 PM

Page 12: [3] Deleted Microsoft Office User 1/24/24 8:42:00 AM

Page 12: [3] Deleted Microsoft Office User 1/24/24 8:42:00 AM

Page 12: [4] Deleted Microsoft Office User 1/24/24 8:43:00 AM

Page 12: [4] Deleted Microsoft Office User 1/24/24 8:43:00 AM

Page 12: [5] Deleted Microsoft Office User 1/24/24 8:43:00 AM

Page 12: [5] Deleted Microsoft Office User 1/24/24 8:43:00 AM

Page 12: [5] Deleted Microsoft Office User 1/24/24 8:43:00 AM

Page 12: [5] Deleted Microsoft Office User 1/24/24 8:43:00 AM

Page 18: [6] Deleted Microsoft Office User 1/24/24 10:15:00 AM

Page 18: [6] Deleted Microsoft Office User 1/24/24 10:15:00 AM

Page 18: [7] Deleted Donaghy, Erin Elizabeth 1/17/24 7:11:00 PM

Page 18: [7] Deleted Donaghy, Erin Elizabeth 1/17/24 7:11:00 PM

Page 18: [7] Deleted Donaghy, Erin Elizabeth 1/17/24 7:11:00 PM

Page 18: [8] Deleted Microsoft Office User 1/24/24 10:15:00 AM

Page 18: [8] Deleted Microsoft Office User 1/24/24 10:15:00 AM

Page 18: [8] Deleted Microsoft Office User 1/24/24 10:15:00 AM

Page 18: [8] Deleted Microsoft Office User 1/24/24 10:15:00 AM

Page 18: [9] Deleted Donaghy, Erin Elizabeth 1/17/24 7:11:00 PM

Page 18: [9] Deleted Donaghy, Erin Elizabeth 1/17/24 7:11:00 PM

Page 18: [9] Deleted Donaghy, Erin Elizabeth 1/17/24 7:11:00 PM

Page 18: [10] Deleted Microsoft Office User 1/24/24 10:16:00 AM

Page 18: [10] Deleted Microsoft Office User 1/24/24 10:16:00 AM

Page 18: [11] Deleted Microsoft Office User 1/16/24 8:49:00 AM

Page 18: [11] Deleted Microsoft Office User 1/16/24 8:49:00 AM

Page 18: [11] Deleted Microsoft Office User 1/16/24 8:49:00 AM

Page 18: [11] Deleted Microsoft Office User 1/16/24 8:49:00 AM

Page 18: [11] Deleted Microsoft Office User 1/16/24 8:49:00 AM

Page 18: [11] Deleted Microsoft Office User 1/16/24 8:49:00 AM

Page 18: [12] Deleted Donaghy, Erin Elizabeth 1/13/24 11:50:00 PM

Page 18: [12] Deleted Donaghy, Erin Elizabeth 1/13/24 11:50:00 PM

Page 18: [13] Deleted Donaghy, Erin Elizabeth 1/14/24 11:39:00 AM

Page 18: [13] Deleted Donaghy, Erin Elizabeth 1/14/24 11:39:00 AM

Page 18: [13] Deleted Donaghy, Erin Elizabeth 1/14/24 11:39:00 AM

Page 18: [13] Deleted Donaghy, Erin Elizabeth 1/14/24 11:39:00 AM